7-1983

Predicting Infiltration and Surface Runoff from Reconstructed Spoils and Soils

Digital Object Identifier: https://doi.org/10.13023/kwrri.rr.143

Larry G. Wells
University of Kentucky, larry.wells@uky.edu

Andrew D. Ward
University of Kentucky

Ronald E. Phillips
University of Kentucky

RESEARCH REPORT NO. 143

PREDICTING INFILTRATION AND SURFACE RUNOFF FROM RECONSTRUCTED SPOILS AND SOILS

BY

Larry G. Wells
Principal Investigator

Andrew D. Ward
Research Associate

Ronald E. Phillips
Cooperating Investigator

1983

UNIVERSITY OF KENTUCKY
WATER RESOURCES RESEARCH INSTITUTE
LEXINGTON, KENTUCKY

United States Department of the Interior
Agreement Number: 14-34-0001-1229 (FY 1981)
P.L. 95-467

RESEARCH REPORT NO. 143

PREDICTING INFILTRATION AND SURFACE RUNOFF FROM RECONSTRUCTED SPOILS AND SOILS

by

Larry G. Wells
Principal Investigator

Andrew D. Ward
Research Associate

and

Ronald E. Phillips
Cooperating Investigator

Project Number: B-078-KY (Completion Report)

Agreement Number: 14-34-0001-1229 (FY 1981)

Period of Project: October 1980-April 1983

Water Resources Research Institute
University of Kentucky
Lexington, Kentucky

The work upon which this report is based was supported in part by funds provided by the United State Department of the Interior, Washington, D.C., as authorized by the Water Research and Development Act of 1978. Public Law 95-467.

July 1983

DISCLAIMER

Contents of this report do not necessarily reflect the views and policies of the United States Department of the Interior, Washington, D.C., nor does mention of trade names or commercial products constitute their endorsement or recommendation for use by the U.S. Government.

ABSTRACT

A laboratory system was fabricated to measure infiltration and runoff from spoil and soil profiles constructed in rectangular bins. Construction, calibration and operation of a rainfall simulator is discussed and instrumentation used to measure transient infiltration and transmittance of water through experimental profiles is described.

Spoil and soil materials from surface mines in Eastern and Western Kentucky were transported to the laboratory and used in constructing experimental profiles in rectangular bins (0.91 x 1.83 x 1.07 m). An extensive series of infiltration experiments were conducted utilizing a rainfall simulator and soil moisture monitoring instrumentation. A dual probe gamma density gauge was used to measure moisture content and tensiometers were used to measure soil matric suction. Initial moisture content, bulk density and rainfall rate were varied and respective responses of infiltration characteristics determined.

Extremely low infiltration rates in Western Kentucky spoil material was attributed to relatively high bulk densities and well-graded particle constituency. Conversely, extremely high infiltration rates were observed for Eastern Kentucky shale material even at very high bulk densities. The sandstone material, however, exhibited infiltration rates of the same order of magnitude as that of Western Kentucky spoil material.

Soil water characteristic curves were developed using the Brooks-Corey and Gardner procedures, based upon desortpion tensiometer data. Unsaturated hydraulic conductivity values were determined using the "plane of zero flux" procedure and compared with predictions resulting from models described by Campbell, Burdine and Mualem for situations involving "reconstructed" soil and spoil materials. There was generally good agreement between the models and "plane of zero flux" results, and excellent agreement with Campbell's predictions.

The infiltration process was modeled with the SCS curve number method, a modified form of Holtan's equation, the Green-Ampt model and Richard's equation. SCS curve numbers were determined by fitting the method to the observed results. Richards' equation gave very good estimates of the infiltration process through the spoil profiles, but was only slightly better than the

Green-Ampt model. None .of the models worked well for the profiles where macropore flow occurred through a two layer topsoil over spoil system.

DESCRIPTORS: Infiltration*, Infiltration Rate*, Infiltration Capacity, Runoff*, Runoff Rates, Soil Water, Soil Water Potential

IDENTIFIERS: Spoils, Spoil Water, Spoil Water Potential

ACKNOWLEDGEMENTS

The authors are grateful for the support and cooperation of Peabody Coal Company and Mr. James Powell in providing material for use in this study. Appreciation is expressed to Island Creek Coal Company and Mr. Richard Bielicki for similar assistance in obtaining material from Eastern Kentucky.

The authors would also like to acknowledge the assistance of Dr. R. I. Barnhisel, who helped obtain the spoil material; George Day, who helped design and construct the infiltrometer system; and Farhad Ravani, who conducted most of the tests on the Eastern Kentucky profiles.

TABLE OF CONTENTS

LIST OF TABLES

LIST OF ILLUSTRATIONS

LIST OF ILLUSTRATIONS (Continued)

NOMENCLATURE

a	A constant.
b	The slope of the log-log plot.
f	The infiltration rate.
f_c	Final steady infiltration rate.
F	The accumulated infiltration.
F_s	Volume of infiltration at time of surface ponding.
I_s	Initial abstraction.
K	The hydraulic conductivity.
K_r	The relative hydraulic conductivity.
K_s	The saturated hydraulic conductivity.
k_f	The relative hydraulic conductivity.
L	The depth of the control zone.
L	The depth to the wetting front from the surface.
P	The accumulated runoff.
Q	The accumulated runoff.
S	The potential maximum retention.
S	The potential storage in the "control" zone.
S	The capillary suction at the wetting front.
S_{w2}	The capillary drive at the wetting front in the subsurface soil.
S_e	Effective saturation.
t	Time.
t_s'	The time required to infiltrate a volume equivalent to F_s under ponded surface conditions.
T_p	The void volume of a "control" zone.
z	The distance below the surface.
ϕ	The matric suction (cm).
ψ	The pressure head.
θ	The soil moisture content (cm/cm).
θ_s	The soil moisture content at effective saturation.
ψ_e	The air entry matric suction.
θ_r	The residual water content (cm^3/cm^3).
ϕ_e	The air entry matric suction (cm).
λ	The pore-size distribution index.
θ_i	The initial moisture content.

CHAPTER I - INTRODUCTION

The objectives of the study were:

1) To determine infiltration parameters for reconstructed spoils and soils
2) To evaluate the capability of existing infiltration models to predict infiltration through reconstructed soil profiles
3) To develop and verify a design model for predicting infiltration parameters based on spoil and soil physical characteristics, ground cover, soil and spoil stratification and surface topography
4) To determine SCS curve number values for reconstructed lands.

Recent worldwide energy shortages have precipitated increased coal mining operations. Improved technology has resulted in a substantial increase in the area of land mined by surface methods. To prevent irreversible damage to these disturbed watersheds, stringent regulations have been placed on the surface mining industry. The authors of these regulations have maintained that protection of the environment of disturbed lands will required a sound understanding of the hydrologic balance of the affected watersheds.

One of the major components of the hydrologic balance is infiltration. The ability of water to move into and through a soil profile has a direct effect on many of the other components of the hydrologic cycle. Estimation of surface runoff depends on accurate characterization of infiltration into the soil and the success of revegetation of these denuded areas will be greatly influenced by the available moisture in the reclaimed profiles.

This report presents the results of a large-scale laboratory study on infiltration through reconstructed spoils and soils from surface mines in Eastern and Western Kentucky.

CHAPTER II - RESEARCH PROCEDURES

Experimental Apparatus

To meet the objectives of the study an infiltrometer system was constructed at the Agricultural Engineering Department at the University of Kentucky. While a brief discussion of the system is presented here, the reader is referred to Ward et al (1) for details.

The infiltrometer system consists of a rainfall simulator and two instrumented soil bins. The system was designed to satisfy the following performance requirements:

1) Generate rainfall rates of 0.5 - 3.5 cm/hr.
2) Generate drop size distribution similar to natural rainfall.
3) Generate rainfall with a similar kinetic energy to natural rainfall.
4) Permit a minimum of 2-4 tests per week.
5) Provide a surface area and depth of sufficient magnitude such that the soil/spoil profile would be representative of field conditions.
6) Incorporate an instrumentation system capable of measuring rapid changes in soil suction throughout the profile.
7) Incorporate an instrumentation system which would measure changes in soil moisture during an infiltration event.

The rainfall simulator for the infiltrometer system was based on a design reported by Brakensiek et al. (2). The system consists of three 0.61 x 0.92 m modules which utilize a two-compartment system of air and water. Each module contains 96 needles with internal diameters of 0.4 to 0.7 mm. The drop sizes are controlled by the air flow rate through the lower module compartment. Air blows down through a small orifice around each needle and shears the drops falling from the needle into a spray of finer drops. The kinetic energy of the drops falling onto the surface of a profile is 70-90 percent of that of natural rainfall.

Two rectangular bins are used to contain the various experimental spoil/soil profiles. The bins are supported 0.73 m above the floor to permit raising and lowering of a dual probe gamma density gauge from the underside of the bins, thus minimizing interference with simulated rainfall (see Figure 1).

Two major monitoring systems are used; a gamma probe to measure soil/spoil density and monitor changes in soil water content and a tensiometer

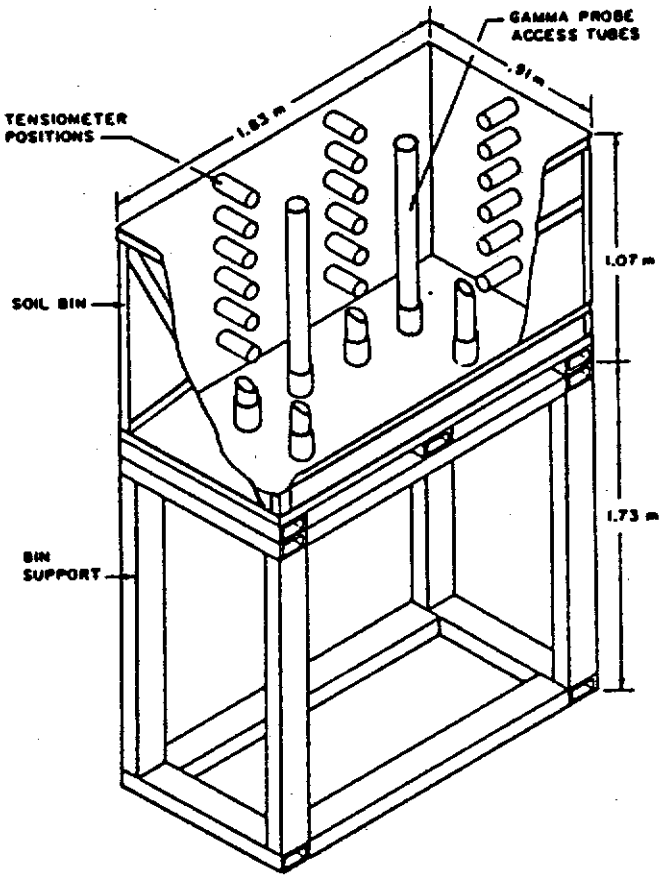

Figure 1. Illustration of Soil Bins and Supports.

network to measure changes in soil water suction. Four tensiometers are centered between gamma probe access tubes within six horizontal planes at various depths in each bin. The first level of tensiometers are positioned in a horizontal plane 15.24 cm below the top of the bin or approximately 7.6 cm below the soil/spoil surface. Each subsequent layer is located at 15.24 cm intervals (see Figure 1).

Tensiometers in a vertical plane are staggered so that the top one is inserted the shortest distance and the bottom tensiometer is inserted the furthest distance. Positioning is such that the soil/spoil above each ceramic cup is uninterrupted.

Density and water content is measured in the bins using a Troxler two-probe gamma density gauge with a CS-137 source. The source and detector are mounted vertically in a pair of guide tubes set on 30.48 cm centers (see Figure 1). The detector counts gamma photons passing rhorugh a pyramid with a rectangular base of 1.27 x 3.81 cm and a height of 30.48 cm. The system, therefore, gives an estimate of the density of a 1.27 cm deep strata of soil between the two guide tubes. By knowing the initial moisture content of the soil, the instrument can be used to measure changes in soil water content and bulk density.

Experimental Procedures and Characteristics of Experimental Profiles

The Western Kentucky spoils and soils were collected from a surface mine in Ohio County in August, 1980. The topography consists of rolling hills with narrow valleys and elevations ranging from 400-500 feet. Surface mining was occurring on the No. 9 coal seam which is in the Carbondale formation of the Pennsylvania System. The strata dips gently to the south and overburden consists mostly of sandstone and grey shale with soderite modules. Topsoil collected at this site was a mixture of Belknap and Sadler silt loams.

The Eastern Kentucky spoils were collected from a surface mine in Martin County in October, 1981. The topography is typical of Appalachia and coal was being mined from the Upper Richardson, Lower Richardson and Broas seams from within the Breathitt Formation of the Carboniferous Pennsylvanian System. Separate samples of sandstone and shale material were transported to the laboratory.

Profile Construction and Characteristics

The bins were packed with soil and spoil materials to form profiles similar to those found in reclaimed areas of the mine sites. A total of 10 profiles were constructed; six (6) from Western Kentucky material and four (4) from Eastern Kentucky material.

To measure changes in moisture content with the gamma probe it was necessary to determine the void ratio of the profiles at each position on the monitroing grid. Void ratios were calculated based on the procedure recommended by Rawls and Brooks (3). Initial moisture contents were determined using gravimetric procedures. These results were then used to determine the void ratios, and subsequent moisture contents were detemined with the gamma probe.

To check the calculated void ratios and soil moisture contents, samples were taken from gravimetric analysis at the end of a test cycle on a profile. Gamma probe estimates were always found to be within 10 percent of the gravimetric determinations of the moisture content. The specific gravity of the materials was determined using standard procedures (4). The specific gravity of the soil and spoil material from Western Kentucky were determined to be 2.72 and 2.68, respectively, and 2.60 for both the shale and sandstone spoils of Eastern Kentucky.

Physical and Chemical Properties of the Materials

An extensive laboratory testing program was conducted to establish the physical and chemical properties of the materails. Tests were conducted by Commonwealth Technology, Inc. and the Agricultural Engineering Department. In general, standard procedures were followed for all the tests. A detailed description of the procedures used is presented by Ward (5). Particle size distribution for the materials were determined at the Agricultural Engineering Department.

Soil Water Characteristics

Relationships between the soil water potential and the moisture content were determined using a procedure described by Gardner (6) for desorption data. The relationship between the soil moisture content and the matric suction is given by the equation

$$\phi = \phi_e(\theta/\theta_s)^{-b} \qquad (1)$$

where ψ is the matric suction (cm), θ is the soil moisture content (cm/cm), θ_s is the soil moisture content at effective saturation, ψ_e is the air entry matric suction and b is the slope of the log-log plot. The procedure is valid only if the desorption data plots as a straight line on a log-log scale. To convert desorption data to absorption data, the x-intercept is divided by 1.6. The desorption data was obtained from the soil suction tensiometer data and gamma probe data which was soil suction tensiometer data and gamma probe data which was recorded at the beginning of each infiltration test, and also from drying tests which were conducted to determine unsaturated hydraulic conductivity of some of the soil/spoil profiles.

An alternative model was described by Brooks and Corey (7) and is given by the equation

$$\psi = \psi_e \left[\frac{\theta - \theta_r}{\theta_s - \theta_r} \right]^{1/\lambda} \qquad (2)$$

where θ_r is the residual water content (cm^3/cm^3), ψ_e is the air-entry matric suction (cm), and λ is the pore-size distribution index. The term $[(\theta - \theta_r)/(\theta_s - \theta_r)]$ is often referred to as the effective saturation, S_e. Mualem's procedure (8) was adopted to determine θ_r and λ. This procedure requires that the dispersion of the measured points around the extrapolated curve passing through the measured last point (ψ_{min}, θ_{min}) should be a minimum for soil water content values ranging between the measured last point and the inflection point. It should be noted that if an inflection point is present, the Mualem procedure is used only to determine θ_r. A second analysis is then conducted to determine ψ_e and λ (Brakensiek et al., 9).

Hydraulic Conductivity

Unsaturated hydraulic conductivity relationships were determined by Campbell's method (20). Campbell's equation for estimating unsaturated hydraulic conductivity is as follows:

$$K_r = \frac{K}{K_s} = \left(\frac{\theta}{\theta_s} \right)^{2b+3} \qquad (3)$$

where K_r is the so-called relative hydraulic conductivity, K_s is the hydraulic conductivity at effective saturation, K is the unsaturated hydraulic conductivity at the moisture content θ, and b is the slope term from equation 1.

Two alternatives to the Campbell model which incorporate the Brooks-Corey soil water characteristic model (equation 2) were described by van Genuchten (10). The first procedure is based upon theory presented by Burdine (11). The relative hydraulic conductivity is determined from the following expression

$$K_r = \left[\frac{\theta - \theta_r}{\theta_s - \theta_r}\right]^{3+2/\lambda} = S_e^{3+2/\lambda} \qquad (4)$$

where K_r is the relative hydraulic conductivity (K/K_s) and all the other terms are as described previously.

The second procedure is obtained by combining the theory presented by Mualem (8) with equation (2). Mualem's theory may be expressed as

$$K_r = S_e^{1/2}\left[\int_0^{S_e}\frac{dS_e}{\psi}\Big/\int_0^{1}\frac{dS_e}{\psi}\right]^2 \qquad (5)$$

Then by combining equations (5) and (2) the following expression for determining the relative conductivity is obtained

$$K_r = \left[\frac{\theta - \theta_r}{\theta_s - \theta_r}\right]^{2.5 + 2/\lambda} = S_e^{2.5 + 2/\lambda} \qquad (6)$$

The relative conductivity term, K_r, in equation (4), (5) and (6) is a function of the effective satuation, S_e.

Steady-state infiltration tests were used to estimate hydraulic conductivity at apparent saturation for Western Kentucky spoil material and dense spoil over spoil. Apparent saturation for these profiles was estimated as 91 and 85 percent of total porosity, respectively.

So-called "plane of zero flux" (PZF) (12) drying tests were conducted on various profiles constructed from Western Kentucky topsoil and spoil material. To develop the hydraulic head versus depth relationships the average soil water content for each 5 cm increment in depth was calculated and a suction corresponding to this water content was obtained from the appropriate soil water characteristic curve. The average soil water content at each 5 cm increment was determined by taking the readings at the point of interest and 2.5 cm either side of the point. The average soil water content for each increment represented the average 9-15 readings, since 3-5 readings were

taken at each level. Where similar results were determined at several depth locations for a particular monitoring time, average values of the hydraulic conductivities and soil water contents, respectively, were determined. At least two PZF drying tests were conducted on each bin. Each test had a duration of 90-120 hours and consisted of scanning the bins at 2.5 cm depth increments using the gamma probe 4 to 7 times during the test. All the hydraulic conductivity values were calculated based on upward gradients of the water from the PZF.

Infiltration Tests

One of the main objectives of the study was to evaluate the influence of the rainfall intensity, initial moisture content, and bulk density on infiltration through a reconstructed soil/spoil profile. Tests were conducted at rainfall intensities of 1-3 cm/hr for profiles constructed from Western Kentucky materials and at intensities of 3-32 cm/hr for profiles constructed from Eastern Kentucky materials. Initial soil/spoil moisture contents ranged from air dry to field capacity. A total of ten different soil/spoil profiles were evaluated.

At the beginning of each infiltration test, the gamma probe was used to determine initial moisture conditions in a profile. Scans were made every 2.54 cm down the profile to a depth of 30-40 cm. At the end of each infiltration test, the final soil moisture content was determined by again conducting a scan of all the points on the selected monitoring grid. Transient soil moisture movement during an infiltration test was monitored with the gamma probe located in one of the sets of access tubes. The gamma probe was then moved down the profile in conjunction with the advance of the wetting front. Between movements, readings were taken, at the same location, every few minutes. Soil moisture contents behind the wetting front were determined by monitoring the grid locations above the wetting front every 30-60 minutes.

Accumulated infiltration was determined by taking the difference between the initial and final moisture contents for a profile as determined by the gamma probe. The infiltration rate during a test was determined by measuring runoff rates from the soil surface. This approach assumes that the rainfall rate is constant, that all of the rainfall is applied to the soil surface, and that the surface storage is small. The approach also provided another measurement of the accumulated infiltration volume.

The duration of each event was controlled so that the wetting front would pass beyond either the first or second level of tensiometers. The test durations ranged from 75-600 minutes depending on soil/spoil type and the density of the profile.

Infiltration Models

The SCS curve number method, a modified form of Holtan's equation, the Green-Ampt model, and Richards' equation were selected for evaluation because they are widely used, and have each been included in surface mine hydrology models. The Green-Ampt model (13) and Richards' equation (Smith and Woolhiser 14) are based on the physics of soil water movement, while the SCS curve number procedure (15) and Holtan's equation (16) are empirical models which have parameters with little or no physical significance.

SCS Curve Number Method

The procedure was developed for small watersheds and was intended for use where only watershed data and daily rainfall records were available. The data used to develop the method was obtained from experimental plots for agricultural soils and agricultural land treatment measures (15). The equation for the method is:

$$Q = \frac{(P - I_a)^2}{(P - I_a) + S} \qquad (7)$$

where Q is the accumulated runoff, P is the accumulated rainfall, S is the potential maximum retention and I_s represents initial abstractions. All quantities are expressed as inches or cm on the watershed.

The maximum potential storage is commonly related to the initial abstractions, I_a, by the relationship:

$$I_a = 0.2S \qquad (8)$$

To facilitate graphical representation of equation (7), S was then related to a curve number, CN, by the relationship:

$$CN = \frac{25400}{254 + S} \qquad (9)$$

where S is expressed in time.

Holtan Model

Holtan (16) and Holtan et al. (17) proposed an empirical equation

based on storage concepts for describing the infiltration process. The infiltration rate is expressed as a function of the available storage above an impeding layer and a final steady infiltration rate. Higgins and Monke (18) modified Holtan's model to give:

$$f = f_c + a \quad (S - F)/T_p^{\ b} \qquad (10)$$

where f is the infiltration rate, f_c is final steady infiltration rate, F is the accumulated infiltration, S is the potential storage in the "control" zone and T_p is the void volume of a "control" zone. Rates are expressed in in/hr or cm/hr and volumes are expressed in inches or centimeters. The "control" depth is defined as the depth to the impeding layer. An evaluation of the 'a', 'b', and 'f_c' values for four soils reported in the study by Higgins and Monke (18) indicated that 'a' was 5-6 times 'f_c' and 'b' could be approximated by 0.65. By substituting these results into equation (10) the equation becomes:

$$f = f_c + 5f_c\,[(S - F)/T_p]^{0.65} \qquad (11)$$

where a in equation (10) is approximated as $5f_c$.

If the steady state infiltration rate is approximated by the field saturated hydraulic conductivity K_{fs}, and total saturation is assumed to occur at a field saturated moisture content, θ_{fs}, then equation (11) can be written as:

$$f = K_{fs} + 5K_{fs}\,[((\theta_{fs} - \theta_i)L - F)/L\theta_{fs}]^{0.65} \qquad (12)$$

where θ_i is the initial moisture content and L is the depth of the control zone. The modified model is thus written in terms of soil physical characteristics.

To overcome problems associated with determining the control depth, a two stage solution of equation (12) was developed. The subscripts 1 and 2 denote the surface and subsurface layers, respectively. Definitions are the same as for the modified GAML model and reference should be made to Figure 2. The two-stage solution is expressed as follows:

$$\text{Stage 1:} \quad f = K_1 + 5K_1\,[((\theta_{s1} - \theta_{i1})L_1 - F/L_1\theta_{s1}]^{0.65} \qquad (13)$$

if $f > i$, then $f = i$ (infiltration rate - rainfall rate)

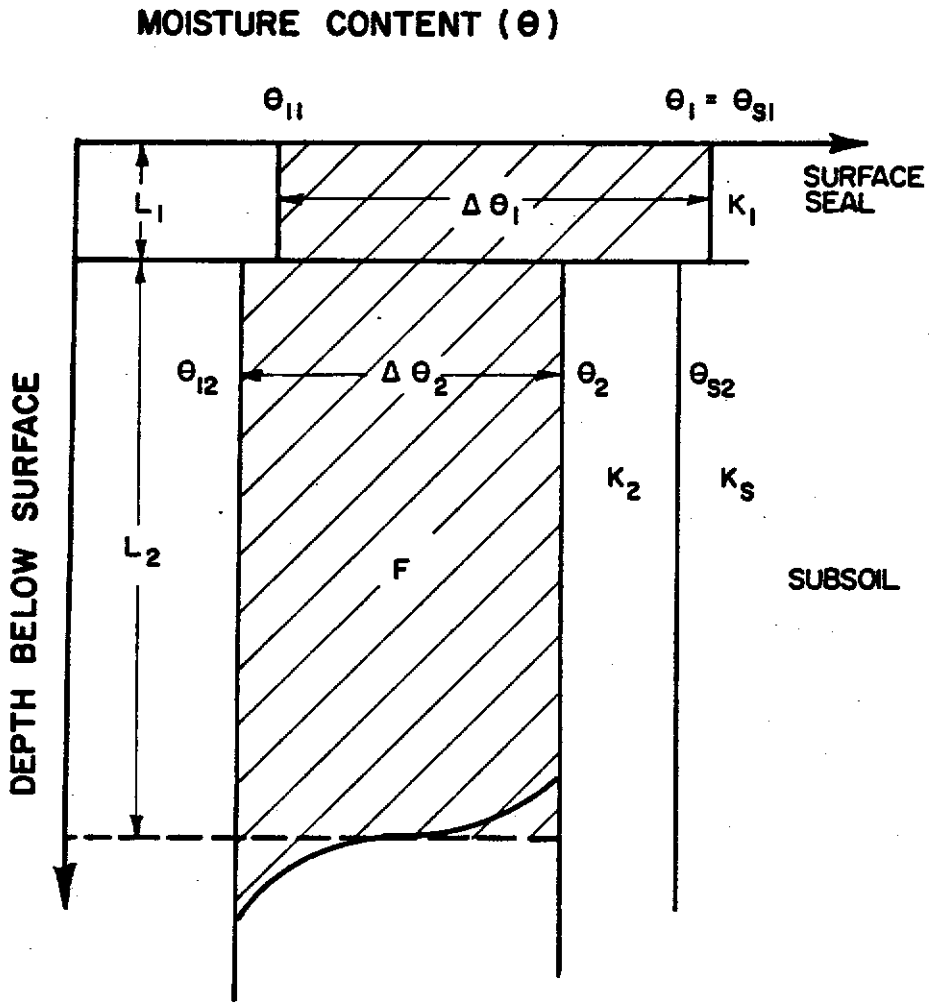

Figure 2. Conceptual Moisture Profile for Derivation of Modified GAML Equation (Source: Moore, 20)).

Stage 2: The surface layer becomes saturated and equation (12) reduces to $f - K_1$. Then:

$$f = K_2 + 5K_2 [(\Delta\theta_2 L_2 - F - \Delta\theta_1 L_1)/L_2\theta_{s2}]^{0.65} \quad (14)$$

where $\Delta\theta_2 = (\theta_{s2} - \theta_{i2})$ and $\Delta\theta_1 = (\theta_{s1} - \theta_{i1})$. If $K_2 > K_1$, then $K_2 = K_1$. This procedure allows infiltration into the unsaturated subsoil and assumes that the layer with the lower conductivity controls infiltration.

Green-Ampt Model

Green and Ampt (13) developed an infiltration equation for ponded surfaces based on Darcy's law and a capillary-tube analogy. This equation can be written as:

$$f = K_s[(L + S)/L] \quad (15)$$

where S is the capillary suction at the wetting front, L is the depth to the wetting front from the surface, K_s is the saturated hydraulic conductivity of the wetted zone, and f is the infiltration rate.

Mein and Larson (19) modified the Green-Ampt model to account for infiltration prior to surface ponding. Their two-stage infiltration model is described by two equations. Stage 1, up to the time of surface ponding, t_s, is described by:

$$F_s = \frac{S(\theta_{fs} - \theta_i)}{[(I/K_{fs}) - 1]} \quad (16)$$

where F_s is the volume of infiltration at the time of surface ponding. At the time of surface ponding, the infiltration rate is equal to the rainfall rate and $t_s = F_s/I$. The second stage of infiltration is described by:

$$K_{fs}(t - t_s + t_s') = F - S(\theta_{fa} - \theta_i)\ln[1 + F/S(\theta_{fs} - \theta_i)] \quad (17)$$

where t_s' is the time required to infiltrate a volume equivalent to F_s under ponded surface conditions.

Moore (20) developed a solution of the GAML model for a two-layer soil profile. A conceptual soil profile for the procedure is illustrated in Figure 2. If Darcy's law is applied to the system and the depth of ponding is negligible, f is determined as:

$$f = \frac{L + S_{w2}}{\frac{L_1}{K_1} + \frac{L_2}{K_2}} \quad \text{for } L \geq L_1 \tag{18}$$

where S_{w2} is the capillary drive at the wetting front in the subsurface soil. At time, t, the volume of water infiltrated is:

$$F = L_1\Delta\theta_1 + L_2\Delta\theta_2 \tag{19}$$

By substituting f = dF/dt into equation (18) and combining equations (18) and (19), the following expression for dF/dt is obtained:

$$\frac{dF}{dt} = \frac{L_1 + \frac{F - L_1\Delta\theta_1}{\Delta\theta_2} + S_{w2}}{\frac{L_1}{K_1} + \frac{F - L_1\Delta\theta_1}{\Delta\theta_2 K_2}} \tag{20}$$

If equation (2) is integrated between the limits $t = t_1$ $(F = F_1)$ and $t = t$, the following expression for the infiltration process is obtained:

$$F + (E - H)\ln\left(1 + \frac{F - F_1}{H}\right) = K_2(t - t_1) + F_1 \tag{21}$$

where $E = L_1\Delta\theta_2(K_2/K_1)$; $H = \Delta\theta_2 (L + S_{w2})$; and $F_1 = L_1\Delta\theta_1$.

Equation (21) is the form of the Green-Ampt equation for single stage infiltration through a two-layer system. For the GAML model for two-stage infiltration through a two-layer system, the equation can be written in the same form as Equation (18).

$$F + (E - H)\ln\left(1 + \frac{F}{(H - F_1)}\right) = K_2(t - t_s + t_s') \tag{22}$$

where F_s is given by the equation:

$$F_s = \frac{H - E\frac{I}{K_2}}{\frac{I}{K_2} - 1} + F_1 \tag{23}$$

Equation (23) applies if F_s exceeds the storage volume in the surface layer. If $L_s > L_1$, equation (16) is used with parameter estimates for the surface layer. The procedure is well suited to solution by computer and the model developed by Moore (20) was used in this study.

Richards' Equation

A computer model described by Moore and Eigel (21) was used in this study to provide a finite difference solution of the one-dimensional form of Richards' equation for a non-swelling soil (Smith and Woolhiser 14):

$$\frac{\partial\theta}{\partial t} + \frac{\partial}{\partial z}\left[K_s k_r(\phi)\frac{\partial\phi}{\partial z}\right] - \frac{\partial[K_s k_r(\phi)]}{\partial z} \qquad (24)$$

where θ is the volumetric moisture content, K_s is the saturated hydraulic conductivity, $k_f(\phi)$ is the relative hydraulic conductivity, ϕ is the pressure head, z is the distance below the surface, and t = time.

A more convenient form of equation (24) is:

$$c\frac{\partial\phi}{\partial t} = \frac{\partial}{\partial z}\left[K_s k_r(\phi)\frac{\partial\phi}{\partial z}\right] - \frac{\partial[K_s k_r(\phi)]}{\partial z} \qquad (25)$$

where c is the moisture capacitance $\partial\theta/\partial\phi$. This equation has no exact general analytical solution. The equation is a second-order, non-linear partial differential equation for unsaturated flow in a porous media where air moves under negligible pressure gradients. An implicit Crank-Nicolson finite difference scheme was used to provide a solution to equation (25).

Predictions of infiltration volume versus time relationships were determined using each of the models and were compared to the observed results from the infiltration tests for the 6 soil profiles comprising the Western Kentucky soil and spoil material.

CHAPTER III - DATA AND RESULTS

Physical, Chemical and Hydraulic Properties of Experimental Soil/Spoil Profiles

Bulk density determinations for each of the experimental profiles are compiled in Table 1. Density of spoil material is within the range of commonly reported values for surface mine areas. Topsoil material varied from highly compacted to moderately compacted.

Table 2 presents the results of various laboratory analyses conducted on the spoil material collected from Eastern and Western Kentucky. The high conductivity of Western Kentucky spoil was associated with the formation and leaching of salt from the profile. Such leaching did result in increased infiltration capacity within these profiles.

Figure 3 shows the results of particle size determinations for the various materials studied. Both the shale and sandstone materials from Eastern Kentucky were considerably coarser than the shale material from Western Kentucky. As expected, the topsoil material was composed of the finest particle sizes.

Table 3 presents the estimates of parameters for various models used to depict the soil water characteristic and unsaturated hydraulic conductivity relationships. Values of r^2 for these models ranged from 0.61 to 0.93. Figures 4-11 illustrate the comparison of the models with measured values of matric suction and hydraulic conductivity which were determined using profiles constructed from material from Western Kentucky. In general, the models investigated described hydraulic properties of these material satisfactorily.

Infiltration Experiments

Western Kentucky Profiles

Typical infiltration results from the Western Kentucky profiles are presented in Figure 12. In Figure 12(a) the transient infiltration rates during each of the tests conducted with air dried initial moisture conditions are presented. All three of the topsoil/spoil profiles exhibited much higher infiltration rates and longer times to surface ponding than the three spoil profiles. The tests conducted on the spoil profiles (tests 1, 5, and 27) show higher infiltration rates initially for the profiles with the lower bulk densities (Profiles 1 and 2) at the surface. Final infiltration rates for these three profiles are similar for these three tests.

Table 1. Profile Physical Characteristics

Profile	Material	Depth (cm)	Void Ratio Mean	Void Ratio Deviation	Bulk Density Mean (g/cm^3)	Bulk Density Deviation
1	Shale[1]	0.0 - 15.2	0.535	0.072	1.750	0.084
		15.2 - 30.5	0.638	0.065	1.639	0.070
		30.5 - 45.7	0.530	0.058	1.754	0.067
2	Shale[1]	0.0 - 15.2	0.562	0.063	1.719	0.072
		15.2 - 30.5	0.539	0.072	1.745	0.082
		30.5 - 45.7	0.563	0.091	1.720	0.106
3	Topsoil[1]	0.0 - 15.2	0.856	0.134	1.474	0.110
	Shale[1]	15.2 - 30.5	0.587	0.073	1.692	0.077
		30.5 - 45.7	0.563	0.091	1.720	0.106
4	Shale[1]	0.0 - 15.2	0.449	0.061	1.853	0.081
		15.2 - 30.5	0.499	0.063	1.790	0.076
		30.5 - 45.7	0.530	0.058	1.754	0.067
5	Topsoil[1]	0.0 - 15.2	0.980	0.138	1.380	0.101
	Shale[1]	15.2 - 30.5	0.540	0.068	1.743	0.077
		30.5 - 45.7	0.563	0.091	1.720	0.106
6	Topsoil[1]	0.0 - 15.2	0.878	0.121	1.455	0.100
	Shale[1]	15.2 - 30.5	0.506	0.070	1.783	0.084
		30.5 - 45.7	0.530	0.058	1.754	0.067
7	Shale[2]	0.0 - 15.2	0.416	0.100	1.848	0.133
		15.2 - 30.5	0.517	0.098	1.719	0.099
		30.5 - 45.7	0.570	0.149	1.668	0.133
8	Sandstone[2]	0.0 - 15.2	0.456	0.075	1.790	0.093
		15.2 - 30.5	0.570	0.123	1.666	0.122
		30.5 - 45.7	0.524	0.095	1.713	0.105
9	Shale[2]	0.0 - 15.2	0.394	0.111	1.876	0.146
		15.2 - 30.5	0.272	0.088	2.053	0.135
		30.5 - 45.7	0.344	0.106	1.945	0.149
10	Mixture[2]	0.0 - 17.6	0.461	0.098	1.787	0.115
	Sandstone[2]	17.6 - 30.5	0.384	0.093	1.888	0.126
		30.5 - 45.7	0.388	0.059	1.877	0.079

1) Material from Western Kentucky
2) Material from Eastern Kentucky

Table 2. Chemical and Physical Properties Test Results

Test	Units	Western Kentucky		Eastern Kentucky	
		Spoil	Topsoil	Shale	Sandstone
Conductivity	µmhos/cm	5530		333	639
pH (water)		5.3	6.3	8.1	7.3
pH (buffer)		6.6	7.1		
TDS	mg/L	7420		180	467
Iron	mg/L	66		<0.01	0.02
Manganese	mg/L	46		0.08	2.52
Aluminum	mg/L	0.30		<0.1	<0.1
Lead	mg/L	<0.01		<0.01	<0.01
Chromium	mg/L	0.07		<0.01	<0.01
Zinc	mg/L	1.2		0.17	0.04
Nickel	mg/L	0.35		<0.01	<0.01
Sodium	mg/L	46		9.8	11.4
Calcium	mg/L	820		23	101
Magnesium	mg/L	281		7	13.5
Sulfate	mg/L	4880		44	136
Total Nitrogen	kg/ha	1326	1219	125	288
Potential Acidity	t/ha	27.1	0	0	0
Organic Matter	%	2.14	0.74		

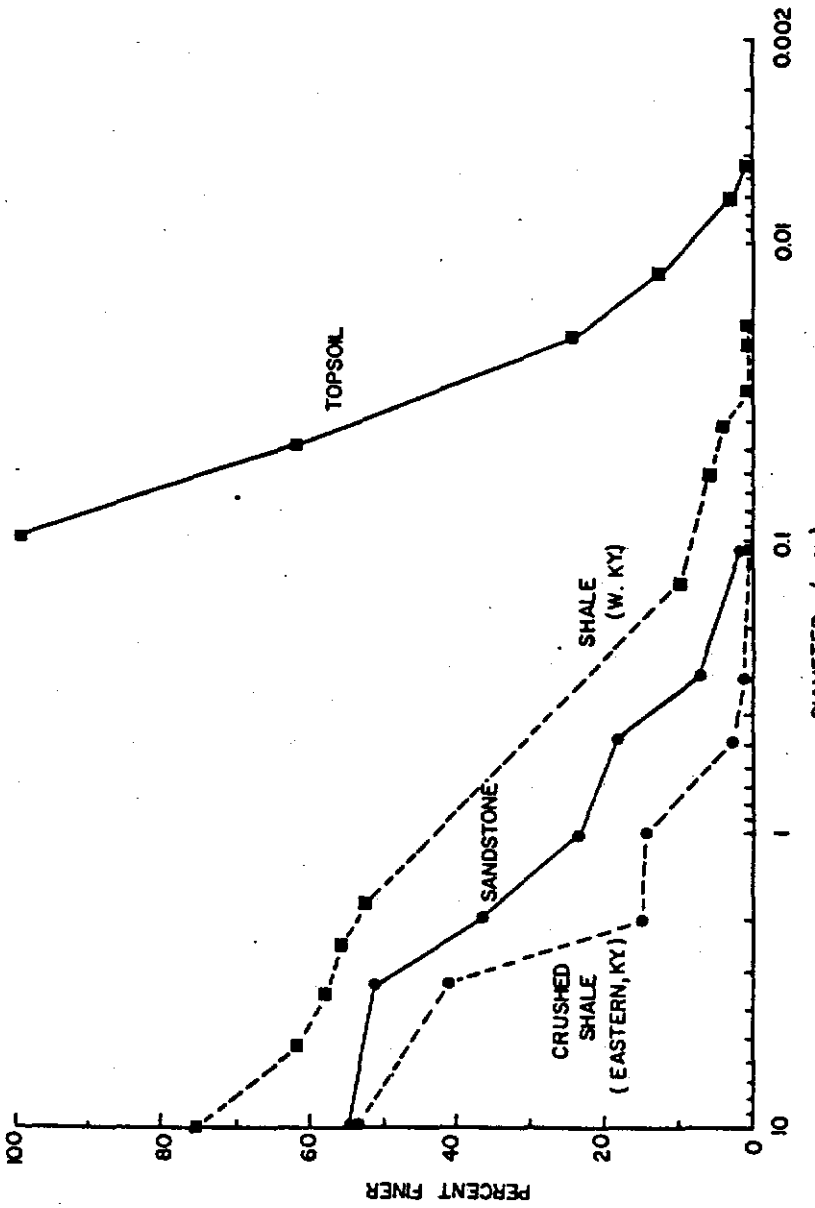

Figure 3. Spoil and Topsoil Particle Size Distribution.

Table 3. Soil Water Characteristic and Hydraulic Conductivity Parameter Estimates

Profile	Material	Porosity (vol/vol)	ψ_e (cm)	ψ_b (cm)	b	λ	2b+3	θ_r	Number Points
1	Shale[1]	0.347	10.53	11.30	5.80	0.33	14.60	0.09	55
2	Shale[1]	0.359	13.31	11.30	4.88	0.33	12.76	0.09	66
3	Topsoil[1]	0.458	3.79	10.10	8.90	0.15	20.80	0.0	7
4	Dense Shale[1]	0.309	17.50	28.9	2.16	0.49	7.16	0.0	19
5	Tilled Topsoil[1]	0.493	6.38	11.9	5.60	0.22	14.20	0.0	21
6	Topsoil[1]	0.465	9.74	11.7	6.03	0.18	15.06	0.0	12
7	Shale[2]	0.318	0.19	-	4.65	-	12.30	-	16
8	Sandstone[2]	0.341	15.03	-	2.10	-	7.20	-	30
9	Dense Shale[2]	0.250	0.18	-	6.82	-	16.64	-	20
10	Sandstone/Shale[2] over Sandstone	0.316	0.85	-	6.02	-	15.04	-	17

1) Western Kentucky

2) Eastern Kentucky

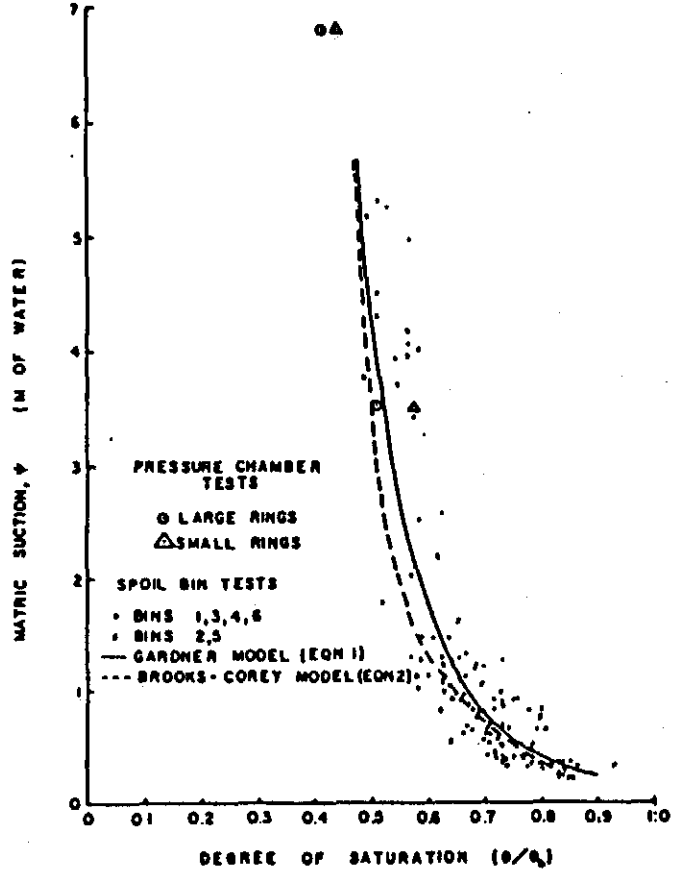

Figure 4. Soil water characteristic relationship (θ vs. ϕ) for all spoil bin horizons except the relatively dense surface layer of profile no. 4.

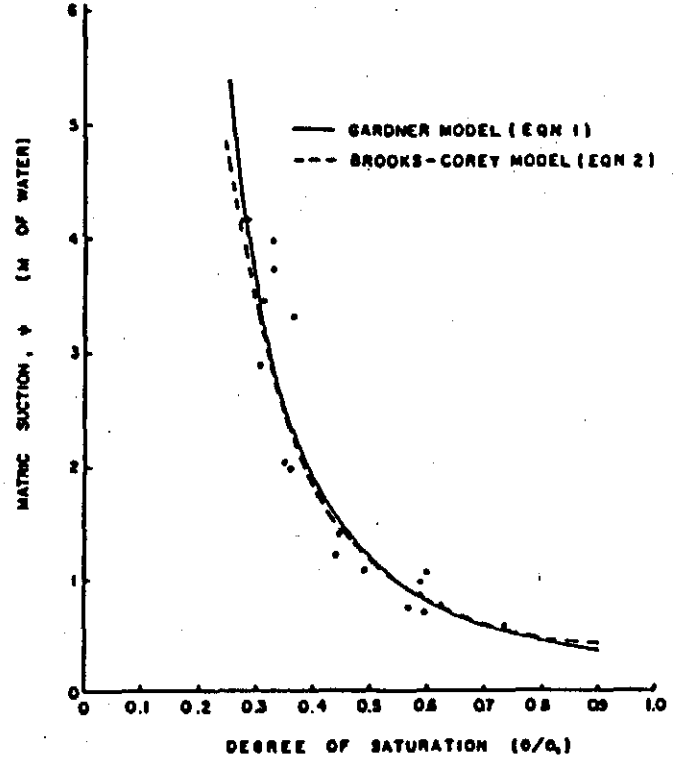

Figure 5. Soil water characteristic relationship (θ vs. ϕ) for the relatively dense spoil surface layer of profile no. 4.

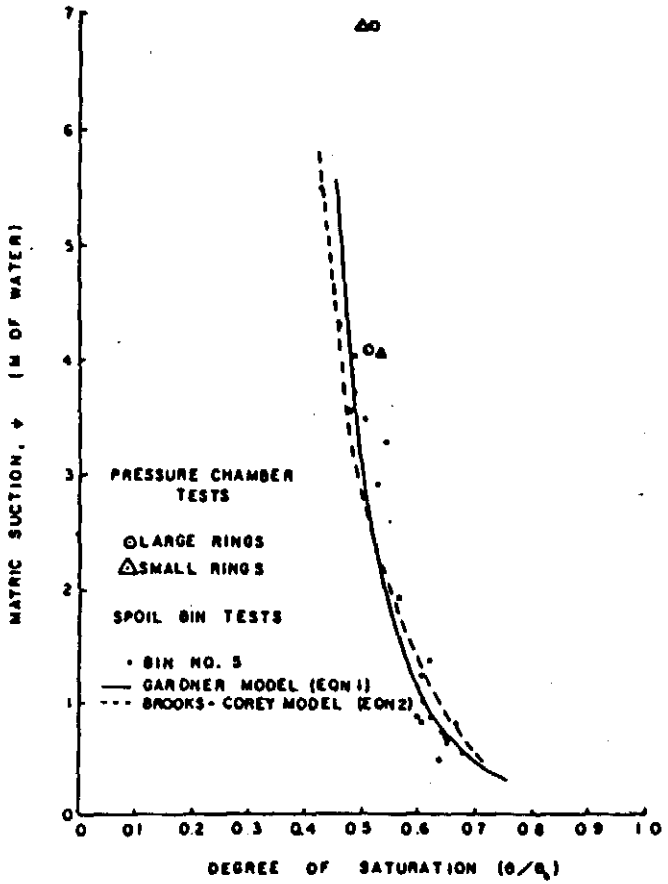

Figure 6. Soil water characteristic relationship (θ vs. ψ) for the topsoil surface layer of profile no. 5.

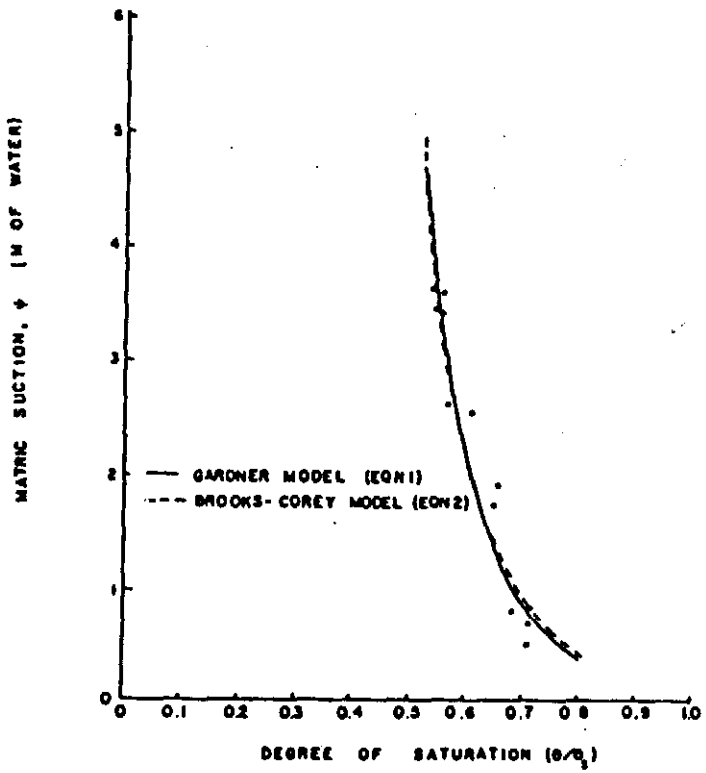

Figure 7. Soil water characteristic relationship (θ vs, ψ) for the relatively dense topsoil surface layer of profile no. 6.

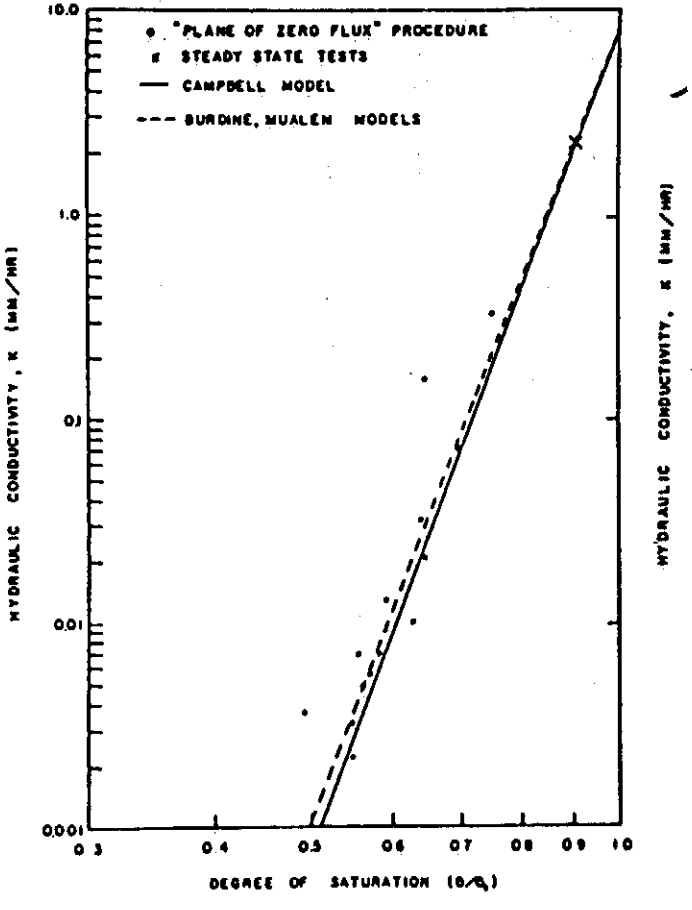

Figure 8. Hydraulic conductivity versus degree of saturation for spoil material comprising profile nos. 1 and 2 (PZF results for profile no. 2 only).

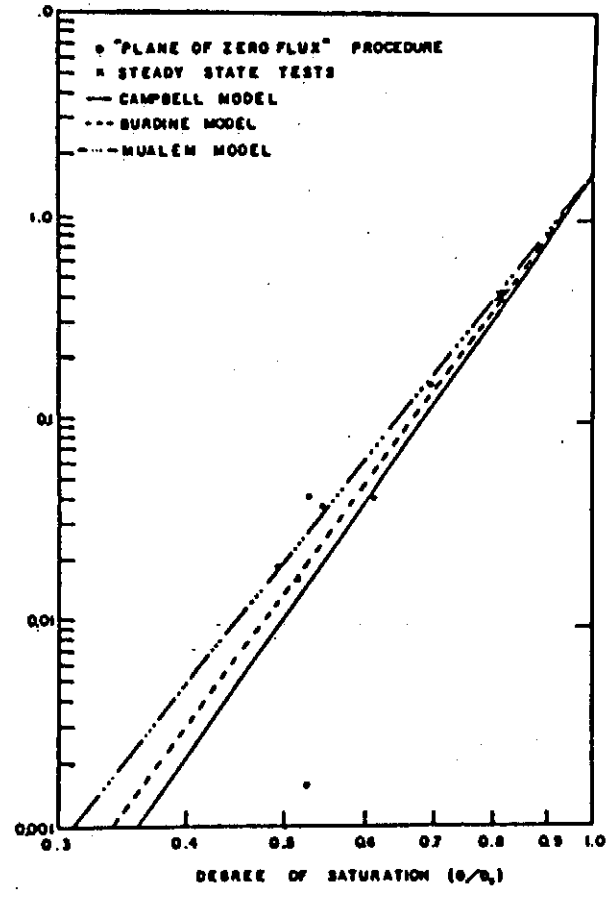

Figure 9. Hydraulic conductivity versus degree of saturation for relatively dense spoil material over spoil material (profile no. 4).

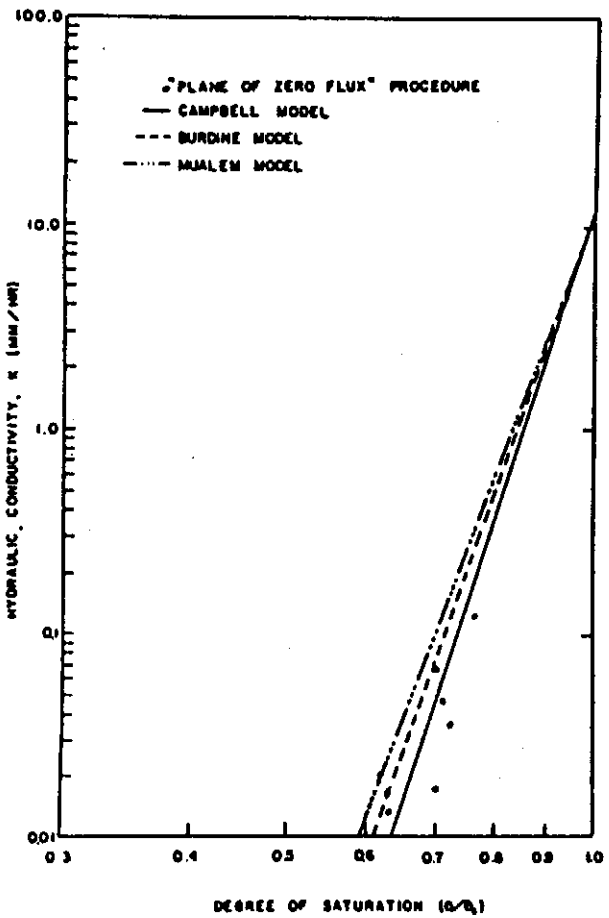

Figure 10. Hydraulic conductivity verus degree of saturation for tilled topsoil over spoil material (profile no. 5).

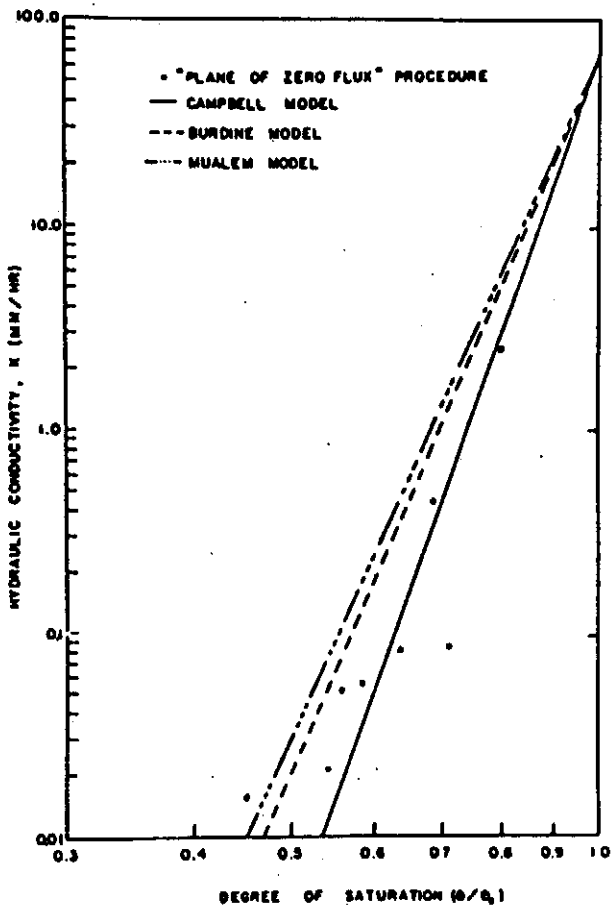

Figure 11. Hydraulic conductivity versus degree of saturation for relatively dense topsoil over spoil material (profile no. 6).

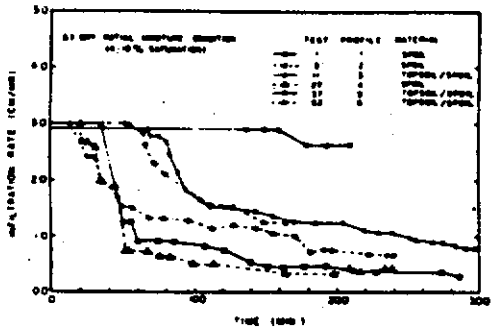

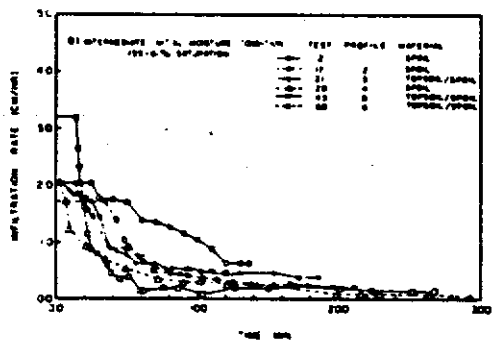

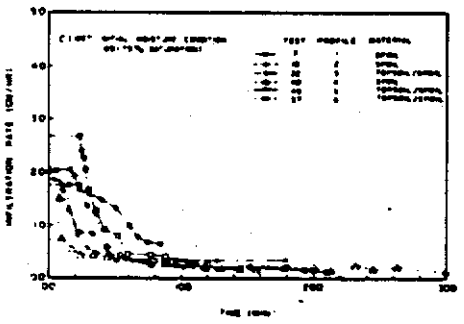

Figure 12. Typical infiltration rate versus time relationships for Western Kentucky Profiles.

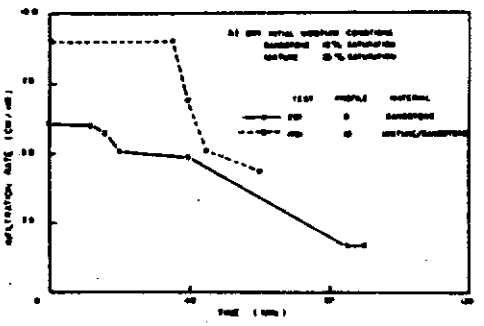

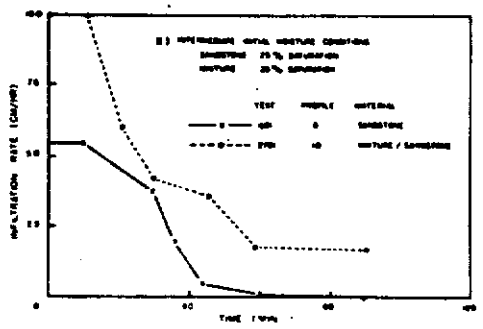

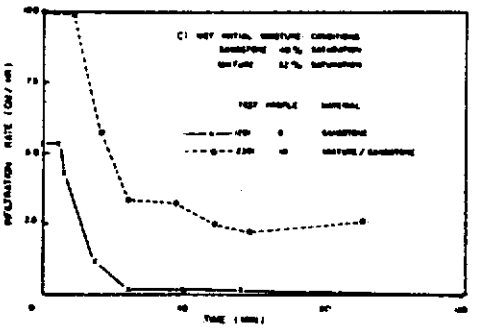

Figure 13. Typical infiltration rate versus time relationships for Eastern Kentucky Profiles.

Figures 12(b) and 12(c) present typical results from the several infiltration tests conducted on each of the profiles at intermediate and relatively wet initial moisture contents for the top 15 cm. Table 4 presents a compilation of information and results for the Western Kentucky profiles. As was the case for dry initial conditions, there is a general agreement in infiltration response between similar profiles (nos. 1 vs. 2 and nos. 3 vs. 6) except for the early stages of the intermediate initial moisture content test where a higher rainfall rate appeared to limit infiltration in Profile no. 1. Additional discussion is presented according to profile types.

Spoil Profiles. It was determined that infiltration through the spoil profiles occurred as a uniform wetting front. For the air dry and intermediate dry initial moisture conditions, the advance of the wetting front could be observed through the plexiglass window. It was noted that when the front reached a pebble or small rock, infiltration would continue to occur on either side of the obstacle, but the area below the obstacle would remain dry for a considerable time. Wetting of the area 1-3 cm below an obstacle appeared to occur through horizontal soil water movement. Movement of the wetting front was also monitored with the gamma probe. Results from the probe indicated that the level of the wetting front in the profile was almost planar at any point in time. Variations in the level of the front at any given time were 0-5 cm. Advance of the front was very slow and never exceeded about 5 cm/hr.

Generally, surface ponding would begin within a few minutes of a test. An analysis of test results indicated that surface ponding generally fell within one-third to one-half of the time to surface runoff. Exact measurement of the time to surface ponding is difficult, as ponding tends to begin to occur in isolated areas and then gradually extends across the profile surface. Complete ponding, however, seldom occurs because high points on the surface tend to be above the elevation at which runoff begins.

For the spoil profiles, ponding occurred farily quickly on all the profiles, indicating that the infiltration process was not substantially limited by the rainfall intensity. For Profiles 1 and 2, the initial infiltration rates decreased to less than 2 cm/hr very shortly after the start of a test except for the two tests conducted with material which was initially air dry. For Profile 4, the initial infiltration rate fell to less than 1 cm/hr (except for the air

Table 4. Western Kentucky Infiltration Results

Test Profile	Test No.	Rainfall Rate (cm/hr)	Test Duration (min)	Degree of Saturation		Time to Surface Ponding (min)	Total Change in Soil Moisture (cm)	Final Infiltration Rate (cm/hr)
				Initial (%)	Final (%)			
1	1	3.05	600	9.4	73.9	11.7 - 17.5	5.89	0.22
	2	3.17	600	57.1	78.0	4.7 - 7.0	1.99	0.06
	4	1.02	480	57.8	79.1	21.0 - 31.5	1.52	0.08
	6	1.02	480	61.0	83.5	19.7 - 19.5	1.84	0.12
	10	0.91	240	59.9	81.5	28.7 - 43.0	1.28	0.07
	3	3.30	540	61.8	83.5	1.0 - 1.5	2.47	0.19
	7	2.67	210	63.7	84.8	7.7 - 11.5	1.36	0.12
2	5	3.05	240	7.5	81.4	8.7 - 13.0	4.91	0.68
	8	2.79	360	35.9	77.6	7.3 - 11.0	2.66	0.25
	12	2.79	210	52.9	76.3	5.0 - 7.5	1.50	0.14
	20	2.67	270	49.7	84.3	10.3 - 15.5	2.56	0.16
	25	2.67	270	51.9	85.4	9.0 - 13.5	2.44	0.23
	33	2.54	180	48.7	76.2	11.3 - 17.0	1.88	0.32
	9	2.79	160	43.0	78.9	7.3 - 11.0	1.58	0.19
	14	2.03	255	49.3	84.4	10.3 - 15.5	2.50	0.31
	17	2.03	210	54.6	83.4	9.0 - 13.5	1.97	0.22
	26	1.88	180	57.9	84.9	10.3 - 15.5	1.80	0.32
	30	2.03	320	54.3	88.8	9.3 - 14.0	3.65	0.24
	15	2.03	240	77.2	90.4	6.3 - 9.5	1.82	0.35
	18	1.93	180	75.8	88.5	5.0 - 7.5	1.50	0.23
	28	1.88	180	68.8	84.9	11.0 - 16.5	1.26	0.27
	34	2.03	150	69.7	82.0	7.3 - 11.0	1.24	0.17
3	11	2.92	300	3.9	88.2	22.7 - 34.0	8.06	0.84
	16	2.92	180	60.0	83.4	3.7 - 5.5	2.60	0.29
	19	2.03	180	63.7	80.8	2.0 - 3.0	1.86	0.26
	21	2.03	180	61.9	80.9	2.0 - 3.0	1.87	0.38
	13	2.92	180	69.7	85.1	3.3 - 5.0	1.90	0.34
	23	2.54	180	76.1	83.9	0.7 - 1.0	0.91	0.37
	22	2.03	180	76.2	85.5	1.0 - 1.5	1.17	0.33
	24	2.03	125	73.3	83.4	1.0 - 1.5	0.93	0.35
4	27	3.05	240	20.7	67.7	7.0 - 10.5	2.58	0.43
	29	2.03	330	41.8	68.7	1.3 - 2.0	1.33	0.09
	31	1.93	330	44.2	67.4	1.0 - 1.5	1.32	0.08
	39	1.93	240	43.0	68.4	1.3 - 2.0	1.32	0.21
	35	1.14	360	43.1	68.7	0.3 - 0.5	1.40	0.14
	44	1.27	360	39.7	70.7	3.3 - 3.5	1.73	0.16
	49	2.92	300	44.7	69.6	2.7 - 4.0	1.26	0.20
	32	1.93	240	66.9	80.3	0.7 - 1.0	0.87	0.28
	40	2.03	300	67.5	78.4	0.3 - 0.5	0.91	0.13
	36	1.14	240	69.4	77.8	0.7 - 1.0	0.65	0.14
	46	1.27	270	64.9	76.2	0.7 - 1.0	0.89	0.05
	51	2.54	240	69.0	78.1	0.7 - 1.0	0.82	0.17
5	37	2.92	210	4.9	59.6	46.0 - 69.0	8.35	2.65
	41	2.03	135	54.1	80.1	18.0 - 27.0	3.28	0.89
	43	2.03	135	58.3	79.6	8.3 - 12.5	2.54	0.63
	47	2.03	135	54.3	80.0	7.3 - 11.0	2.83	0.96
	54	2.03	140	54.0	81.4	18.3 - 27.5	3.48	0.78
	58	2.03	140	51.6	80.7	20.7 - 31.0	3.49	0.74
	38	2.92	75	71.0	84.7	5.3 - 8.0	1.78	0.52
	42	2.03	80	67.8	81.5	6.7 - 10.0	1.35	0.63
	45	2.03	85	71.2	83.9	5.7 - 8.5	1.24	0.63
	48	2.03	75	63.9	78.4	5.7 - 8.5	1.95	1.46
	50	2.03	80	64.4	80.6	3.3 - 5.0	1.96	0.71
	55	2.03	80	65.2	81.3	7.0 - 10.5	2.07	0.49
	59	2.03	75	68.4	80.5	4.0 - 6.0	1.42	0.46
6	52	3.05	175	10.7	80.8	17.3 - 26.0	5.70	1.26
	56	2.03	120	56.1	79.6	7.3 - 11.0	2.27	0.53
	60	2.03	120	59.4	78.0	4.7 - 7.0	1.90	0.49
	53	2.03	90	75.0	86.7	2.3 - 3.5	1.20	0.49
	57	2.03	120	75.7	83.0	2.3 - 3.5	0.69	0.49
	61	2.03	120	74.9	82.6	0.7 - 1.0	0.99	0.24

dry test) within a few minutes after the start of a test. Average final infiltration rates for the three profiles were estimated as 0.14 cm/hr, 0.22 cm/hr, and 0.04 cm/hr. Estimates for Profiles 2 and 4 were made based on replicated long-duration tests lasting 2-4 days. For Profile 1, the average of the final infiltration rate determined for each of seven infiltration tests (see Table 4) was found to give the estimate of 0.14 cm/hr.

Except in the very early stages of a test, rainfall rate did not have a significant effect on the infiltration process through the single layer spoil profiles. At rates higher than 1.02 cm/hr there was only a very slight reduction in the time to surface ponding during some of the tests. For the three tests on Profile 1, conducted at intensities near 1 cm/hr, the surface ponding time was significantly longer than for the higher rates. The dense spoil profile (Profile 4) exhibited very rapid surface ponding, and the reported ponding times were mainly affected by the microrelief of the surface.

No changes in the total infiltration volume for a test could be attributed to the rainfall intensity. The small influence of the rainfall intensity on the infiltration process is consistent with the saturated hydraulic conductivities for each of the profiles. Maximum influence occurred when the rainfall intensity was similar to the saturated hydraulic conductivity. For this case, however, the rainfall intensity was nearly five times the field saturated hydraulic conductivity. This result, however, is consistent with results reported by Moore (22) and Mein and Larson (19).

With the drying technique used in the study, it was possible to obtain fairly uniform moisture conditions in the top 15-20 cm of a profile. The results showed that the infiltration process was significantly influenced by the initial moisture content of this layer. With an increase in the initial moisture content, there was a marked decrease in initial infiltration rates, time to surface ponding, and total infiltration volume. Reduction in infiltration rates and volume is due to the much lower available fillable porosity and the lower soil suctions associated with the higher initial moisture contents. The results discussed previously showed that the spoil and topsoil materials exhibited very rapid changes in suction and hydraulic conductivity over a very narrow range of moisture contents.

The final moisture content showed a slight influence by initial moisture conditions. For higher initial moisture conditions, higher final moisture

conditions were observed. Although small, this observation was fairly consistent and indicated that air entrapment played a small role in the infiltration process. As the observed influence appeared small in this study, a detailed evaluation of air entrapment effects was not made.

Topsoil/Spoil Profiles. Initial infiltration rates were limited to the applied rainfall rates for all the tests not conducted at a relatively wet initial moisture condition. Infiltration initially occurred as gravity flow through the large cracks at the surface. Between the cracks, a well established 2-5 mm thick surface layer or seal was observed. The sealed areas were preserved from test to test. As a test progressed, the soil around the cracks would swell and the size of the cracks would be greatly reduced. Sediment laden flow across the surface would then result in a sealing of the cracks. This process generally occurred 20-40 minutes after the start of a test.

Rapid wetting front advancement was observed in the profile such that the infiltration process began to be impeded by the underlying spoil layer within 60 minutes of the start of a test. The effect of the surface sealing process was, therefore, masked by the impeding effect of the spoil layer. Tests conducted with the surface scarified (tests 54, 55, 58, and 59) showed significant increases in the volume of infiltration. The time to surface ponding was also increased for the two tests conducted at the dry initial moisture conditions. The results indicated that the degree of surface sealing present at the start of a test played a more significant role than a seal which formed during the event.

For the two-layer topsoil/spoil profiles, flow through the cracks at the surface was very significant. Flow reached the topsoil/spoil interface 15-16 cm below the surface much more rapidly than might be expected with piston flow. With time, the cracks would gradually close and a seal would form at the surface. Until the seal was completely formed, the infiltration process was dominated by flow in the cracks and by the impeding spoil layer. The observed initial infiltration process is very similar to that reported by Quisenberry and Phillips (23) and by Thomas and Phillips (24).

The gradual closing of the cracks and the formation of a seal at the surface is consistent with transient seal concepts. Studies on this topic have been made by Edwards and Larson (25), Whisler et al. (26) and Moore (22). The results of the special tests evaluating the influence of the surface sealing

phenomenon indicated that the surface area initially sealed and the number of cracks were the most significant factors affecting infiltration.

Eastern Kentucky Profiles

Typical infiltration results for the Eastern Kentucky profiles are presented in Figure 13 (refer back). No results are presented for the two shale profiles (7 and 9) as infiltration was always limited to the applied rainfall rate. In Figure 13(a) transient infiltration rates during the two tests conducted with dry spoil material are presented. It should be noted that in test 1701, on the two layer system of a sandstone-shale mixture over sandstone, only the 17 cm thick surface layer of mixed material was dry initially.

A summary of all the infiltration tests on the Eastern Kentucky profiles is presented in Table 5. Figures 13(b) and 13(c) present typical results from the infiltration tests conducted on Profiles 8 and 10 at intermediate and relatively wet initial moisture conditions in the top 15-17 cm, respectively. In general, similar profiles exhibited similar infiltration responses. As with the Western Kentucky profiles, the initial moisture content of Profiles 8 and 10 significantly influenced the time to surface ponding and the rate of decay of the infiltration tests. A further discussion of the results follows.

Shale Profiles. Results of the tests on the shale profiles were inconclusive as the infiltration responses for these profiles were always limited by the applied rainfall rates. Profile 7 consisted of very coarse (pebble size and larger) pieces of shale and gravity flow through the large voids was the major infiltration mechanism. Rapid drainage from the underside of the profile (about 90 cm below the surface) occurred 12-40 minutes after the start of a test, depending on the rainfall intensity. The total changes in soil moisture reported in Table 5 for Profiles 7 and 9 were determined with the gamma probe and tend to be underestimated because of the rapid drainage from the profiles at the end of each test.

Profile 9 was formed by compacting the shale material in Profile 7 and by adding additional compacted material to the profile. In the compaction process the shale pieces were broken into smaller particles (see Figure 3). Gravity flow through the macropore structure was, however, still the dominant infiltration mechanism. Drainage through the underside of the profile occurred at about the same time as for the less dense profile. Very high

Table 5. Eastern Kentucky Infiltration Results

Test Profile	Test No.	Rainfall Rate (cm/hr)	Test Duration (min)	Degree of Saturation Initial (%)	Degree of Saturation Final (%)	Drainage or Ponding Time (min)	Change in Soil Moisture (cm)	Final Infiltration Rate (cm/hr)
						Drainage		
7	101	6.0	90	16.6	34.2	41.0	3.70	6.00
	301	6.0	90	27.3	33.5	29.0	1.22	6.00
	501	6.0	60	27.2	38.3	33.0	2.47	6.00
	701	6.0	60	32.2	40.5	34.0	1.80	6.00
	901	8.0	60	24.6	40.4	21.0	3.46	8.00
	1101	8.0	60	30.1	35.2	19.0	1.21	8.00
	1301	16.0	90	26.1	40.8	18.0	3.25	16.00
	1501	16.0	60	32.4	40.8	12.0	1.73	16.00
						Ponding		
8	201	6.0	90	9.6	53.1	3.0 - 4.5	8.45	1.70
	401	6.0	90	51.8	58.8	2.3 - 3.5	1.40	0.05*
	601	6.0	90	45.2	52.3	5.0 - 7.5	1.68	0.05*
	801	5.4	90	53.7	57.5	3.3 - 5.0	0.78	0.05*
	1001	5.4	120	45.9	53.6	5.0 - 8.5	1.59	0.05*
	1201	5.4	120	52.3	57.3	2.0 - 3.0	1.11	0.05*
	1401	3.1	120	41.4	48.7	4.3 - 6.5	1.51	0.10
						Drainage		
9	1601	9.0	60	38.2	50.9	24.0	2.30	9.0
	1801	13.0	60	44.4	52.8	12.0	1.30	13.0
	2001	13.0	60	45.2	55.1	15.0	1.41	13.0
	2201	13.0	60	44.4	55.6	12.0	1.90	13.0
	2401	24.4	90	40.1	54.6	10.0	2.48	24.4
	2501	32.0	45	44.6	53.0	10.0	1.42	32.0
	2901	16.0	60	35.3	49.8	13.0	2.53	16.0
	3101	16.0	60	43.3	50.5	14.0	1.25	16.0
						Ponding		
10	1701	9.0	60	59.2	75.8	11.7 - 18.5	3.81	4.35
	1901	8.3	90	65.1	77.9	6.0 - 9.0	2.81	3.10
	2101	10.0	90	60.0	71.1	4.7 - 7.0	2.34	3.15
	2301	10.0	90	66.7	72.8	3.0 - 4.5	1.36	2.55
	2701	10.0	90	58.8	69.4	3.7 - 5.5	2.31	1.80
	2801	10.0	90	63.3	71.3	2.0 - 3.0	1.66	4.60
	3001	10.0	90	53.2	65.5	6.3 - 9.5	2.57	6.60**
	3201	9.8	60	56.8	65.4	5.0 - 7.5	1.91	6.60**

* Nominal Estimate. Rainfall Essentially Equal to Runoff

** Rapid Drainage Observed from Underside of the Profile

rainfall intensities were applied to this profile and no surface ponding was observed. Long duration steady state tests were not conducted on the shale profiles because of the inability to obtain rainfall rates of significant magnitude to induce surface runoff. The saturated hydraulic conductivity of the dense shale profile will be greater than 32 cm/hr (maximum rainfall rate applied in Test 2501). This result is consistent with saturated hydraulic conductivities of 14.4-756.0 cm/hr reported by Rogowski and Weinrich (27) for Appalachian surface mine materials.

Sandstone and Sandstone-Shale Profiles. The infiltration response of the sandstone profile (Profile 8) appeared to be controlled by a cementing action at the surface. During the initial test (Test 201) on the freshly packed, relatively dry material the infiltration rates were high and there was a large change in the soil moisture content. In all the subsequent tests surface ponding occurred very rapidly and only small changes in soil moisture occurred near the surface. Surface runoff rates generally approached the applied rainfall rates within 30 minutes and tensiometers located 7-10 cm below the surface showed no changes until 90-120 minutes after the start of rainfall.

Profile 10 was formed by placing 15-17 cm of a mixture of the sandstone and shale material over compacted sandstone material from Profile 8. No cementing action was observed at the surface and infiltration rates were fairly high for all the tests. The results indicate that the saturated hydraulic conductivity of the sandstone sublayer was lower than that of the surface layer consisting of mixed material although this was not established with certainty. A long duration (48 hours) steady state test resulted in a steady drainage rate of cm/hr through the underside of the profile. Significant washing out of sand particles was, however, also observed and seepage down the inside sides of the bins resulted in some experimental error. Seepage and sand washout problems occurred to a lesser extent during all the tests in Profile 10. Based on the final infiltration rates reported in Table 5, it is estimated that the saturated hydraulic conductivity of the mixed layer was greater than 2 cm/hr. These values are substantially lower than the value of 54 cm/hr reported by Rogowski and Weinrich (27) for an Appalachian sandstone spoil. It is possible, however, that the sandstone used in their study consists of larger particles and was thus coarser in nature. The sandstone used in Profiles 8 and 10 contained very few pebbles and rocks and had the

appearance of a coarse river area in Minnesota, Wislon et al. (28) reported final infiltration conductivities used with three infiltration models in that study ranged between 5-6 cm/hr for the Sverup loamy sand. These results are very similar to the results obtained in Profiles 8 and 10 when surface cementing did not occur.

Infiltration Models

Curve numbers were determined for each test by using measured rainfall and runoff volumes and equations (9) and (10). As the initial abstraction term in the SCS procedure includes surface storage, the runoff data results were used in the analysis. A regression analysis was conducted with the curve number results to develop a model for estimating curve numbers based on physical properties of a profile. Bulk density, total porosity, degree of saturation, and the initial volumetric soil moisture content (at the start of a test) were used in the analysis. The most statistically significant model can be expressed as:

$$CN = 145.8 - 231.2(\theta_s - \theta_i) - 47.0(\theta_i/\theta_s) \qquad (26)$$

where θ_i is the initial soil moisture content (vol/vol) and θ_s is the saturated soil moisture content or total porosity (vol/vol). The $(\theta_s - \theta_i)$ term is a measure of the fillable porosity, and the (θ_i/θ_s) term is a measure of the degree of saturation. The coefficient of determination (r^2) for the equation is 0.83 and all the parameters are significant at the 99.99 percent level. Average θ_i and θ_s values for the top 15 cm of a profile were used in the analysis.

An analysis was conducted with equation (26) to determine how well it predicted the infiltration volumes for the 61 tests. Observed rainfall volumes were used in conjunction with curve numbers determined with equation (26). Runoff and infiltration volumes were then calculated with equation (7). The predicted infiltration results are presented in Table 6.

Table 7 is a compilation of infiltration model parameters determined for Western Kentucky materials. Observed versus predicted accumulated infiltration volume resulting from the Holtan, Green-Ampt and Richards' procedures are shown in Figures 14-16, respectively. Stable solutions were not obtained with Richards' equation for the air dried tests. For most of the topsoil/spoil two layer profile tests it was necessary to model surface sealing

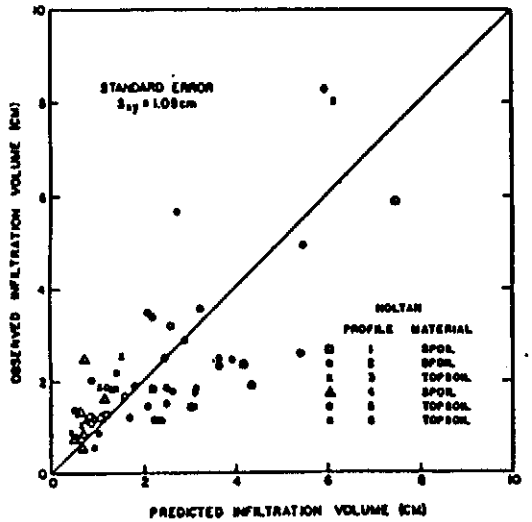

Figure 14. Observed versus Predicted Infiltration Volumes. Holtan Model Results

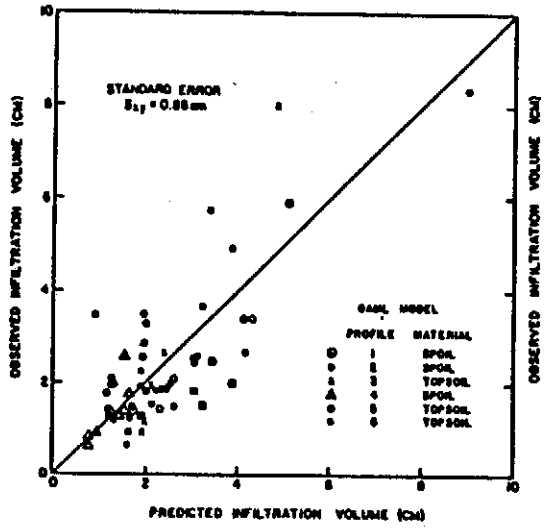

Figure 15. Observed versus Predicted Infiltration Volumes. GAML Model Results

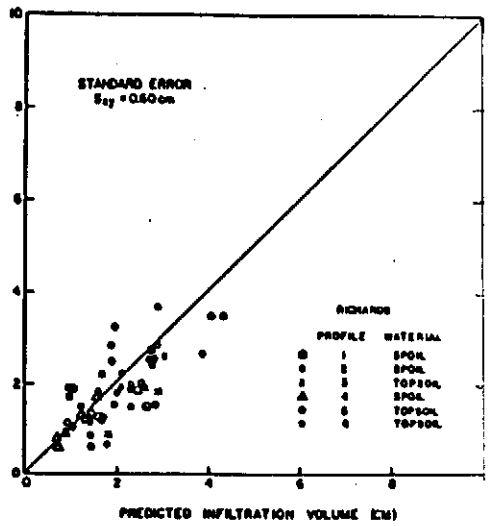

Figure 16. Observed versus Predicted Infiltration Volumes. Richards' Equation Results

Table 6. Accumulated Infiltration Value Estimates

Profile	Test	Gamma Probe (cm)	Runoff Data (cm)	SCS[1] CN	SCS[2] CN	SCS (cm)	Holtan (cm)	GAML (cm)	Richard (cm)
				Spoil Profiles					
1	1	5.89	5.80	73.0	68.6	4.88	7.49	5.08	-
	2	1.99	2.55	84.3	82.7	2.08	4.53	3.88	3.10
	3	2.47	3.04	79.4	84.8	1.62	4.18	3.47	2.74
	4	1.52	2.43	86.0	82.1	1.90	3.02	3.25	2.65
	6	1.84	2.35	85.9	84.8	1.66	2.16	3.04	2.09
	7	1.36	2.40	86.7	85.6	1.61	1.27	1.74	1.44
	10	1.28	2.44	83.2	84.5	1.46	2.23	1.90	1.64
2	5	4.91	5.35	61.0	57.8	4.72	5.49	3.88	-
	8	2.66	3.83	74.5	72.1	3.30	5.45	4.19	3.86
	9	1.58	2.10	88.1	79.8	2.10	2.51	2.14	1.98
	12	1.50	2.60	80.6	80.0	2.24	3.03	2.61	2.37
	14	2.50	2.50	84.8	78.3	2.25	3.89	3.03	2.73
	15	1.82	1.75	88.5	91.4	1.13	2.59	2.05	1.66
	17	1.97	2.38	83.9	79.6	2.06	3.13	2.56	2.33
	18	1.50	1.69	86.5	90.7	1.15	2.10	1.71	1.41
	20	2.56	3.87	75.4	80.5	2.47	3.73	3.14	2.89
	25	2.44	2.83	83.9	79.6	2.35	3.66	3.07	2.83
	26	1.80	2.38	83.1	82.2	1.83	2.61	2.24	2.04
	28	1.26	2.42	83.4	87.2	1.42	2.45	1.95	1.71
	30	3.65	3.04	77.4	80.5	2.13	3.27	3.25	2.92
	33	1.88	2.60	87.5	78.0	2.31	2.68	2.48	2.34
	34	1.24	1.19	95.3	87.8	1.35	1.73	1.68	1.44
4	27	2.58	3.60	76.2	70.1	2.63	0.75	1.55	-
	29	1.33	1.72	84.8	78.8	1.85	0.93	1.54	1.47
	31	1.32	2.05	81.3	79.8	1.81	1.10	1.50	1.44
	32	0.87	1.51	86.6	88.9	1.09	0.70	0.87	0.73
	35	1.40	1.42	86.9	79.3	1.74	1.15	1.58	1.51
	36	0.65	0.96	90.3	88.0	1.08	0.72	0.80	0.73
	39	1.32	1.46	86.5	79.3	1.77	0.75	1.27	1.23
	40	0.91	1.47	88.3	89.0	1.11	0.85	0.96	0.90
	44	1.73	1.83	84.4	78.0	1.86	1.18	1.64	1.61
	46	0.89	0.90	91.4	88.0	1.13	0.78	0.99	0.88
	49	1.26	1.97	85.3	79.8	1.88	0.91	1.42	1.37
	51	0.82	1.35	88.1	89.9	1.05	0.64	0.80	0.74
3	11	8.06	8.65	50.6	44.8	9.01	6.05	4.82	-
	13	1.90	2.67	81.1	85.5	2.12	1.05	2.12	2.42
	16	2.60	2.39	83.1	79.0	2.88	1.50	2.37	2.75
	19	1.86	1.80	83.2	81.5	2.14	1.05	2.27	2.65
	21	1.87	2.37	76.0	79.0	2.61	1.39	2.38	2.64
	22	1.17	1.58	84.4	88.5	1.66	0.70	1.96	1.78
	23	0.91	1.56	85.3	89.1	1.64	0.68	1.91	1.85
	24	0.93	1.34	85.8	86.9	1.66	0.49	1.61	1.67
5	37	8.35	10.04	18.8	40.1	8.58	5.86	8.98	-
	38	1.78	2.36	75.8	83.9	1.91	1.56	1.13	1.03
	41	3.28	3.61	67.7	72.7	2.97	2.54	1.95	1.98
	42	1.35	1.91	77.9	81.8	1.80	0.99	1.22	1.04
	43	2.54	3.13	65.9	75.1	2.80	2.47	1.89	1.93
	45	1.24	1.95	76.7	83.4	1.76	0.94	1.23	1.08
	48	1.95	2.13	61.0	79.3	1.85	1.79	1.22	1.06
	50	1.96	1.79	74.3	79.4	1.92	1.30	1.27	1.12
	54	3.48	3.86	64.7	72.7	3.00	2.14	4.17	4.10
	55	2.07	1.84	83.2	80.1	1.88	0.92	2.65	2.59
	58	3.49	3.77	73.7	71.04	3.13	2.11	4.34	4.35
	59	1.42	1.59	82.6	82.2	1.71	0.56	2.34	2.38
	47	2.83	3.33	58.5	68.6	2.96	2.81	1.94	1.94
6	52	5.70	6.09	55.4	47.8	6.70	2.74	3.40	-
	53	1.20	1.39	85.3	87.4	1.47	0.85	1.32	1.12
	56	2.27	2.44	75.4	75.6	2.53	1.42	1.89	1.71
	57	0.69	1.21	89.7	87.6	1.61	0.94	1.59	1.43
	60	1.90	1.90	82.0	78.1	2.36	1.31	1.90	1.65
	61	0.93	0.99	91.4	87.8	1.59	1.04	1.58	1.44

[1] Calculated from observed results.

[2] Calculated using equation 26.

Table 7. Infiltration Model Parameter Estimates

Parameter	Units	Profile 1	Profile 2	Profile 3	Profile 4	Profile 5	Profile 6
No Seal							
θ_{s1}	vol/vol	0.317	0.327	0.461	0.264	0.495	0.468
θ_{s2}	vol/vol	0.333	0.333	0.333	0.333	0.333	0.333
K_1	cm/hr	0.14	0.22	0.20	0.04	1.52	0.20
K_2	cm/hr	0.22	0.22	0.22	0.22	0.22	0.22
S_{w1}	cm water	21.0	21.0	19.8	33.1	16.3	19.8
S_{w2}	cm water	21.0	21.0	21.0	21.0	21.0	21.0
L_1	cm	25.24	25.24	15.24	15.24	15.24	15.24
Surface Seal							
θ_{s1}	vol/vol			0.461		0.495	0.468
θ_{s2}	vol/vol			0.461		0.495	0.468
K_1	cm/hr			0.06		0.06	0.06
K_2	cm/hr			1.00		6.80	1.00
S_{w1}	cm water			19.8		16.3	19.8
S_{w2}	cm water			19.8		16.3	19.8
L_1	cm			0.40		0.40	0.40

when using the Green-Ampt model and Richards' equation. Typical transient infiltration results for the three infiltration models are illustrated in Figures 17-18. Overall the best results were obtained with Richards' equation. The Green-Ampt model gave very similar results to Richards' equation and both models worked well when micropore flow occurred. The performance of all three models for the tests conducted on the two-layer system was not very good. In Figure 18, the Holtan model appears to provide the best estimates but in several of the other tests the other models performed better. None of the models, however, gave good accounts of infiltration through the cracks in the topsoil layer.

Transient infiltration depth results are shown in Figures 19-21. In Figures 19 and 20, the ability of the Richards' equation to predict infiltration into the soil profiles is illustrated, while in Figure 21 the inability of the procedure to model non-Darcian flow through the two layer system is illustrated.

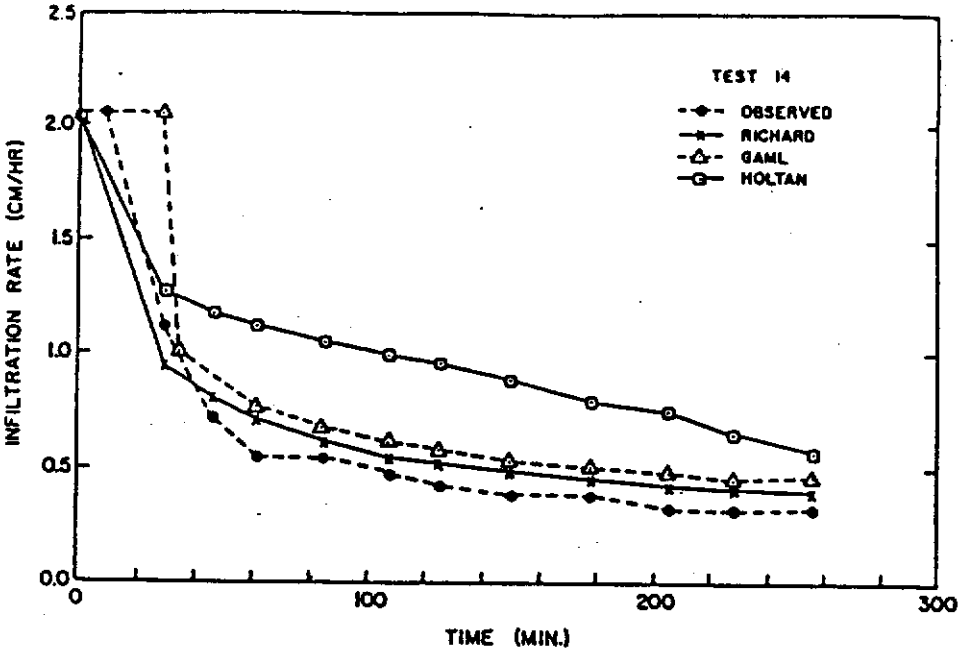

Figure 17. Typical transient infiltration rate estimates for a spoil profile.

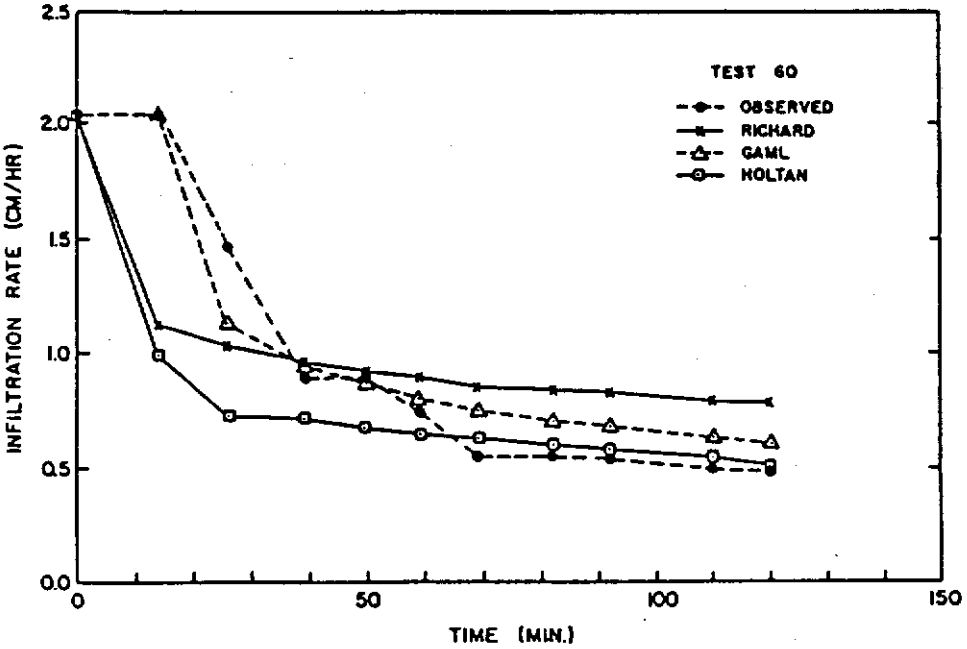

Figure 18. Typical transient infiltration rate estimates for a topsoil/spoil profile.

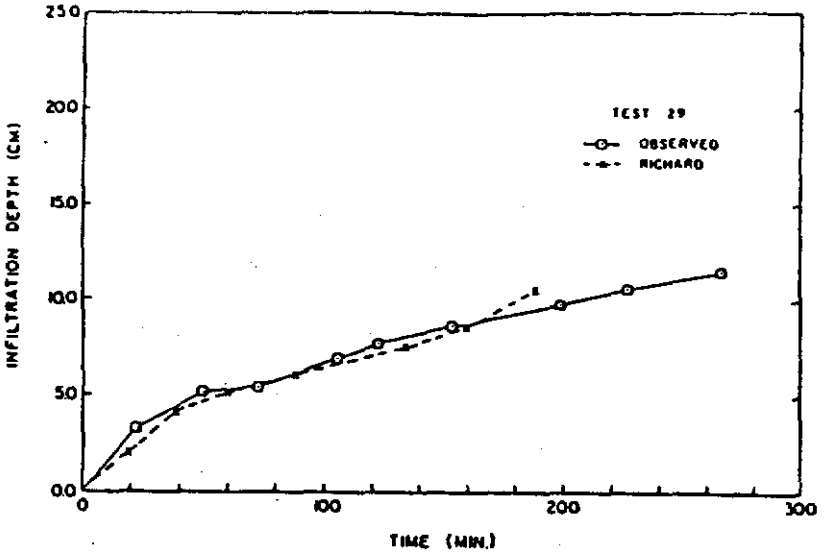

Figure 19. Transient depth of infiltration results for Test 29. (Spoil Profile 4)

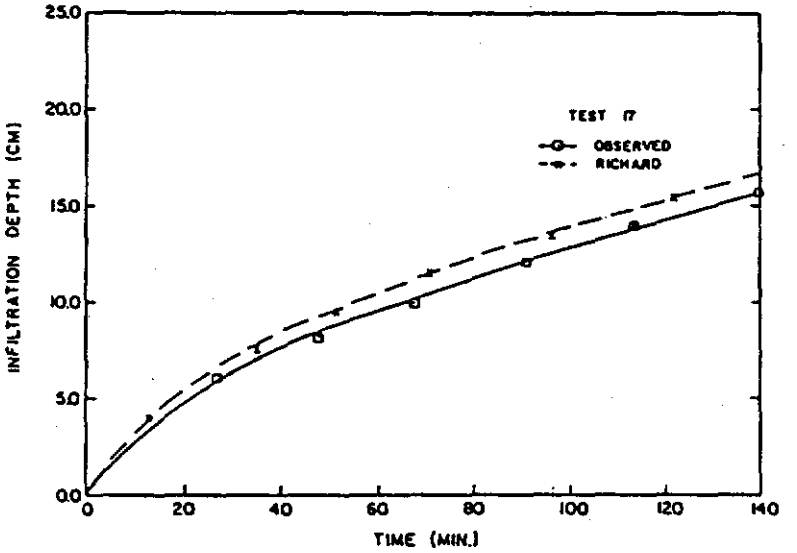

Figure 20. Transient depth of infiltration results for Test 17. (Spoil Profile 2)

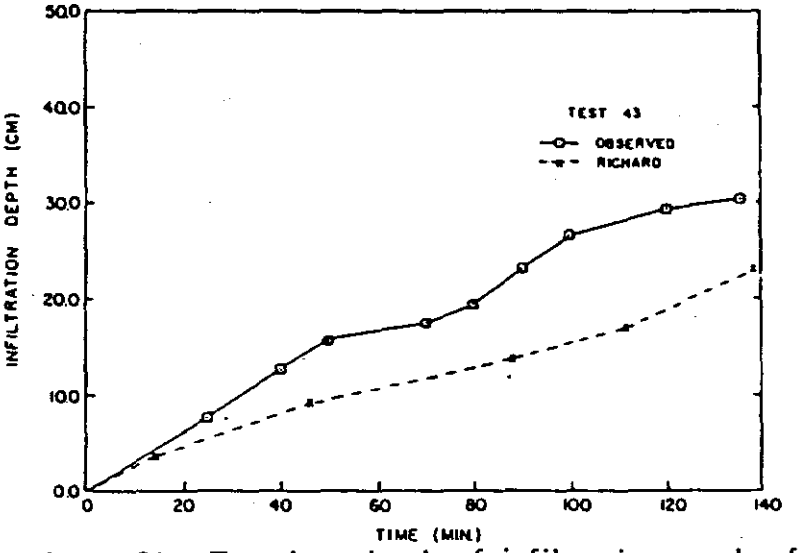

Figure 21. Transient depth of infiltration results for Test 43. (Topsoil/Spoil Profile 5)

CHAPTER IV – CONCLUSIONS

The infiltrometer system used in the study appears to be a viable method for measuring infiltration through reconstructed soil and spoil profiles. For the Eastern Kentucky profiles settlement and redistribution of the spoil profiles was significant and accurate determination of changes in soil moisture was more difficult. Because of the fine spacing of the monitoring grid it is felt that the gamma probe still provided good estimates of bulk density, degree of saturation, and changes in soil moisture. The results of the study are within the wide range of results reported by Rogowski and Weinrich (27), Younis and Shanholtz (29) and McWhorter et al. (30).

Desorption water release relationships for all materials from both Eastern and Western Kentucky were relatively well described as exponential functions of matric suction as given by equation (1). For the Western Kentucky profiles, Campbell's model for describing unsaturated hydraulic conductivity versus soil moisture content was determined effective. The reader is referred to Ward et al. (31) for details concerning hydraulic conductivity relationships. In general, for those profiles which were characterized by diffusion-type flow through micropores. The existence of cracks and large macropores or surface sealing introduced a level of complexity which could not be accounted for using conventional methods of soil hydraulic properties.

Infiltration through the Western Kentucky spoil profiles was characterized by a well-defined wetting front. The extremely low infiltration rates through this shale spoil was attributable to the well-graded particle constituency and the relatively high bulk densities of the profiles. Infiltration through all the other profiles was controlled by the macropore structure of the profile and/or surface effects. Infiltration through the Western Kentucky topsoil horizons was typical of many agricultural soils in which surface sealing occurs.

Despite relatively high densities (2.0 gm/cm^3), the Eastern Kentucky shale profiles had infiltration characteristics which were more typical of a rock landfill than a soil profile. The information obtained with these profiles was limited by the inability (in the laboratory system) to generate rainfall rates which would produce surface runoff. The Eastern Kentucky sandstone and sandstone-shale profiles behaved more like Western Kentucky profiles. Cementing of the sandstone particles at the surface seemed to be the dominant factor influencing infiltration through the sandstone profile. When shale

was mixed with the sandstone this effect was greatly reduced.

Although an extensive series of tests were conducted during this study it is felt that the results should be interpreted with caution. Different geological associations will result in spoil materials with widely different characteristics. Different mining and reclamation techniques might also result in profiles (from the same geological association) with very different infiltration characteristics. In this study the Eastern Kentucky shale material was very coarse and exhibited very high infiltration rates. The authors, however, have observed this same material in the field being crushed and compacted into very dense laeyes of fine well-graded material similar to the Western Kentcky shale material. Corase shale material found in head-of-hollow fills and reclaimed sublayers in Eastern Kentucky might therefore exhibit very different infiltration characteristics from finely compacted material found at the surface of some reclaimed areas. It should also be noted that all the results reported in this report are for a bare soil. Surface sealing effects will probably be substantially influenced by vegetation on the profiles. Salt concentrations were very high for the Western Kentucky profile and appeared to influence infiltration through three profiles. Salt problems were not observed for the Eastern Kentucky materials.

The SCS curve number model gave good estimates of the accumulated infiltration volume for each of the tests. The model was, however, fitted to each of the tests because of a lack of information on curve numbers for strip mine spoils and soils. The goodness of fit, therefore, is misleading. If a single curve number is used for tests with similar initial conditions, the goodness of fit is much worse.

The Holtan Model gave poor estimates of infiltration through the profiles. Performance of the method was slightly better for the topsoil/spoil profiles than for the spoil profiles. The modified model has the advantage over the original Holtan model in that it is based on physical and hydraulic parameters. The results indicated that, with some modifications, the performance of the model might be greatly improved. A wider base is, however, required to develop any further modifications. The current model cannot be recommended for use with surface mine spoils and soils from Western Kentucky.

The modified Green-Ampt model worked fairly well for the spoil horizons

and poorly for the topsoil/spoil horizons. Poor performance for the topsoil/spoil profiles was attributed to the difficulty in determining the model parameters and the non-piston type flow which occurred through this system. Parameters for all the horizons were related to field saturated conditions. For the spoil profiles, establishment of the parameters was straight forward although a knowledge of field saturation conditions was required. For the topsoil/spoil profiles, parameter determination was more complex. An alternative modeling approach (of the infiltration process) might have resulted in a better fit by the model for the topsoil/spoil profiles. The model appears suitable for application in any profile system where piston flow is perceived to occur. The modified model has the advantage over the original model in that it can be applied to a layered system.

The Richards' equation numerical model gave the best estimate of infiltration through the different profiles. For the topsoil/spoil profiles, the model was not better than the GAML or Holtan models. For the spoil profiles, however, the model gave very good estimates of the infiltration process. A major disadvantage of the model was that stable conditions were not obtained for the profiles with very dry initial moisture conditions. The modified GAML results were only slightly worse than the results obtained with the numerical model. It was felt, therefore, that for situations where piston type flow occurred, the modified GAML model could be used instead of Richards' equation.

REFERENCES

1. Ward, A. D., L. G. Wells, and R. E. Phillips. 1981. Infiltration Through Reconstructed Surface Mine Spoils and Soils. Amer. Soc. of Agr. Engrs., Paper No. 81-2508, St. Joseph, Michigan.

2. Barnhisel, R. I., G. Wilmohoff and J. L. Powell. 1979. Characterization of Soil Properties of Reconstructed Prime and Non-Prime Land in Western Kentucky. Proc. Symposium on Surface Mining Hydrology, Sedimentology, and Reclamation, University of Kentucky, Lexington, Kentucky. December 4-7.

3. Rawls, W. J. and R. H. Brooks. 1975. Gamma Probe Dry Bulk Densities. Soil Sci. Vol. 120(1):68-70.

4. Black, C. A. (Ed.). 1965. Methods of Soil Analysis. American Society of Agronomy, Madison, Wisconsin.

5. Ward, A. D. 1981. Characterizing Infiltration Through Reconstructed Surface Mine Profiles. Unpublished Ph.D. dissertation, University of Kentucky, Lexington, Kentucky.

6. Gardner, W. R. 1970. Field Measurement of Soil Water Diffusivity. Soil Sci. Soc. Am. Proc. 341:832-843.

7. Brooks, R. H. and A. T. Corey. 1964. Hydraulic Properties of Porous Media. Hydrology Paper No. 3. Colorado State University, Fort Collins.

8. Mualem, Y. 1976. A New Model for Predicting the Hydraulic Conductivity of Unsaturated Porous Media. Water Resources Research, 12:513-522.

9. Brakensiek, D. L., R. L. Engleman and W. J. Rawls. 1981. Variation Within Texture Classes of Soil Water Parameters. Trans. of ASAE, 24 (2):335-339.

10. van Genuchten, M. rh. 1980. A Closed-Form Equation for Predicting the Hydraulic Conductivity of Unsaturated Soils. Soil Sci. Am. J. 44: 892-898.

11. Burdine, N. T. 1953. Relative Permeability Calculations from Pore Size Distribution Data. Petr. Trans. Amer. Insti. Mining Metall. Eng. 198:71-77.

12. Arya, L. M., D. A. Farrell and G. R. Blake. 1975. A Field Study of Soil Water Depletion Patterns in Presence of Growing Soybean Root: I. Determiantion of Hydraulic Properties of the Soil. Soil Sci. Soc. Amer. Proc. 39:424-436.

13. Green, W. H. and G. A. Ampt. 1911. Studies of Soil Physics. 1. The Flow of Air and Water Through Soils. J. Agric. Sci. 4(1):1-24.

14. Smith, R. E. and D. A. Woolhiser. 1971. Mathematical Simulation of Infiltrating Watersheds. Hydrol. Paper 47, Colorado State Univ., Fort Collins.

15. Soil Conservation Service. 1973. A Method for Estimating Volume and Rate of Runoff in Small Watersheds. SCS-TP-149, U.S. Department of Agriculture, Soil Conservation Service, Washington, D.C.

16. Holtan, H. N. 1961. A Concept for Infiltration Estimates in Watershed Engineering. USDA-ARS Paper No. 41-51.

17. Holtan, H. N., C. B. England and V. O. Shanholtz. 1967. Concepts in Hydrologic Soil Grouping. Trans. ASAE 10:3:407-410.

18. Huggins, L. F. and E. J. Monke. 1967. A Mathematical Model for Simulating the Hydrologic Response of a Watershed. Water Resources Research 4:29-539.

19. Mein, R. G. and C. L. Larson. 1971. Modeling Infiltration Component of the Rainfall-Runoff Process. Bulletin 43, Water Resour. Research Center, University of Minnesota, Minneapolis, Minnesota 72 pp.

20. Moore, I. D. 1981. Infiltration Equations Modified for Surface Effects. Journal of the Irrigation and Drainage Division, ASCE, Vol. 107, No. IR1:71-86.

21. Moore, I. D. and J. D. Eigel. 1981. "Infiltration Into Two-Layered Soil Profiles." Transactions of the American Society of Agricultural Engineers 24(6):1496-1503.

22. Moore, I. D. 1981. Two-Stage Infiltration Equations Modified for Surface Effects. Journal of the Irrigation and Drainage Division, ASCE, Vol. 107, No. IR1:71-86.

23. Quisenberry, V. L. and R. E. Phillips. 1976. Percolation of Surface-Applied Water in the Field. Soil Sci. Soc. Am. J., 40:484-489.

24. Thomas, G. W. and R. E. Phillips. 1976. Consequences of Water Movement in Macropores. J. Environ. Qual., 8(2):149-152.

25. Edwards, W. H. and W. E. Larson. 1969. Infiltration of Water into Soils as Influenced by Surface Seal Development. Trans. Amer. Soc. Agr. Engrg. 12(4):463-465, 470.

26. Whisler, F. D., K. K. Watson and S. J. Perrens. 1972. The Numerical Analysis of Infiltration into Heterogeneous Porous Media. Soil Sci. Soc. Am. J., 36(6):868-874.

27. Rogowski, A. S. and B. E. Weinrich. 1981. Modeling Water Flux on Stripmined Land. Trans. of the ASAE, 24(4):935-940.

28. Wilson, B. N., D. C. Slack and R. A. Young. 1982. A Comparison of Three Infiltration Models. Trans. Amer. Soc. Agr. Engr., 25(2):349-356.

29. Younis, T. M. and V. O. Shanholtz. 1980. Soil Texture and Hydraulic Properties of Post-Mining Soil as Related to the Pre-Mining Soil Horizon. Symposium on Surface Mining Hydrology, Sedimentology, and Reclamation, University of Kentucky, Lexington, Kentucky.

30. McWhorter, D. B., J. W. Rowe, M. W. VanLiew, R. L. Chandler, R. K. Skogerboe, D. K. Sunada, and G. V. Skogerboe. 1979. Surface and Sub-Surface Water Quality Hydrology in Surface Mined Watersheds. Part I. Text EPA Report EPA-600/7-79-193a. Cincinnati, Ohio.

31. Ward, A. D., L. G. Wells, and R. E. Phillips. 1982. Modeling Unsaturated Hydraulic Conductivity of Western Kentucky Surface Mine Horizons. Soil Sci. Soc. Am. J. (In Press).